

Sylvia Heikkilä

CHARACTERIZATION METHODS FOR MASS TRANSPORT IN HYDROGELS

Bachelor's thesis
Faculty of Medicine and Health Technology
April 2022

ABSTRACT

Sylvia Heikkilä: Characterization methods for mass transport in hydrogels
Bachelor's thesis
Tampere University
Faculty of Medicine and Health Technology
Biotechnology and biomedical engineering
4/2022

Hydrogels are manufactured as scaffolds for 3D cell cultures in tissue engineering along with other biomedical applications. Sufficient mass transport is fundamental requirement for scaffold due to the need for necessary exchange of gases, nutrients and waste molecules to cell culture viability. In hydrogels, mass transport is mainly occurring via diffusion and rate of it depends on hydrogel's physical and chemical properties. Characterization of diffusion behaviour in hydrogels is studied commonly with fluorescence methods and is used to develop suitable scaffold materials for 3D cell culturing.

The aim of this literature review is to map methods for diffusion characterization in hydrogels. Different methods are described along with introduction to hydrogels as polymer material and theory background for diffusion in hydrogel network. Transport of molecules can be estimated with diffusion coefficient and value of it determined by tracking the mobility of fluorescent probe molecule or measuring the concentration of diffusive molecule in hydrogel. Mobility of molecules can be detected with measuring changes fluorescence intensities in detection area or volume depending on the method. In addition to fluorescence methods, NMR and Raman spectroscopy approaches to diffusion characterization were introduced. Phenomena in the background of the techniques is briefly discussed for the fluorescence, NMR and Raman spectroscopy methods.

The methods that were introduced in this thesis can be used to study diffusion in different size scales. Transport of molecules in hydrogels can be estimated from measurements in mobility of individual molecules or imaging transport within the whole sample. Additionally, synthetic fluorescent probes are widely used in diffusion characterization studies in modelling the diffusion behaviour within fluorescence methods. It was found that the established diffusion characterization method is in the process to be developed and obtaining accuracy with efficiency needs more research on the current methods or creating new techniques.

Keywords: hydrogel, mass transport, diffusion, cell culture, fluorescence

The originality of this thesis has been checked using the Turnitin OriginalityCheck service.

TIIVISTELMÄ

Sylvia Heikkilä: Diffuusio-ominaisuuksien määrittäminen hydrogeeleissä
Kandidaatintyö
Tampereen yliopisto
Lääketieteen ja terveysteknologian tiedekunta
Bioteknologia ja biolääketieteen tekniikka
4/2022

Hydrogeelejä voidaan käyttää kasvatusalustana kolmiulotteisissa kudosteknologisissa soluviljelmissä. Kasvatusalustassa elävät solut tarvitsevat toimivan vaihdon kaasujen, ravinteiden ja metaboliatuotteiden välillä ja siksi aineensiirto-ominaisuudet ovat yksi tärkeimpiä huomioon otettavia ominaisuuksia kehitettäessä alustoja soluviljelmälle. Hydrogeeleissä aineensiirto tapahtuu pääosin diffuusion kautta ja riippuu hydrogeelin fysikaalisista ja kemiallisista ominaisuuksista. Hydrogeelien diffuusio-ominaisuuksia määritetään enimmäkseen fluoresenssipohjaisilla menetelmillä ja niitä voidaan hyödyntää kolmiulotteisten soluviljelmien kehittämiseen kudosteknologisissa.

Työn tavoitteena on kartoittaa hydrogeelien diffuusio-ominaisuuksien karakterisointimenetelmiä. Työssä kuvataan menetelmiä ja esitellään lyhyesti hydrogeelit materiaaliryhmänä sekä teoriakehys diffuusiolle hydrogeeleissä. Aineiden siirtoa voidaan arvioida diffuusiokertoimen avulla ja sen arvo määrittää tarkastelemalla fluoresoivan molekyylin liikkumista tai mittaamalla diffundoituvan molekyylin pitoisuutta hydrogeelissä. Molekyylin liikkumisesta saadaan tietoa kuvantamalla fluoresenssin intensiteetin vaihtelua tarkasteltavassa alueessa tai tilavuudessa. Työssä esitellään myös NMR- ja Raman -spektroskopiamenetelmät, joilla voidaan selvittää hydrogeelien diffuusio-ominaisuuksia. Menetelmien taustailmiöt ja yksinkertainen teoriakehys esitellään menetelmien kuvailun ohessa fluoresenssi-, NMR-, ja Raman-spektroskopiakäytännöille.

Työssä esiteltyjä menetelmiä käytetään diffuusio-ominaisuuksien tutkimisessa ja niillä saadaan tietoa aineiden liikkeistä eri kokoluokissa. Diffuusiota hydrogeeleissä voidaan tarkastella yksittäisten molekyylien liikkeen kautta tai taltioida liikettä koko näytteessä samaan aikaan. Syneteettisten fluoresoivien kohtamolekyylien käyttö on yleistä diffuusiota mallinnettaessa, kun käytetään fluoresenssipohjaisia menetelmiä. Kirjallisuuskatsauksen perusteella havaittiin, että lisäselvityksiä tarvitaan niin olemassa oleville menetelmille kuin uusien kehittämiseksi. Vakiintunutta menetelmää ei ole vielä muodostunut hydrogeelien diffuusio-ominaisuuksien tutkimisessa ja riittävän tarkan ja tehokkaan menetelmän löytäminen vaatii lisää tietoa ja tutkimuksia.

Avainsanat: hydrogeeli, aineensiirto, diffuusio, soluviljelmä, fluoresenssi

Tämän julkaisun alkuperäisyys on tarkastettu Turnitin OriginalityCheck –ohjelmalla.

CONTENTS

1. INTRODUCTION	5
2. HYDROGELS	7
2.1 Hydrogel properties and structure	7
2.2 Hydrogel synthesis.....	8
2.3 Diffusion in hydrogels.....	10
3. FLUORESCENCE-BASED METHODS.....	13
3.1 Detecting mobility of fluorescein molecule.....	15
3.1.1 Mobility in capillary hydrogels.....	15
3.1.2 Fluorescence recovery after photobleaching.....	17
3.1.3 Fluorescence correlation spectroscopy	22
3.1.4 Optical projection tomography.....	26
3.1.5 Förster resonance energy transfer	27
3.2 Fluorescence sensors	29
4. OTHER METHODS	32
4.1 Raman spectroscopy	32
4.2 Nuclear magnetic resonance.....	34
5. CONCLUSIONS.....	38
REFERENCES.....	41
APPENDIX A: TABLE OF CHARACTERIZATION METHODS	43

LIST OF SYMBOLS AND ABBREVIATIONS

<i>CLD</i>	Crosslinking density
ξ	Mesh size
<i>Q</i>	Equilibrium swelling ratio
<i>SR</i>	Swelling ratio
<i>D</i>	Diffusion coefficient
<i>P</i>	Permeability
<i>S</i>	Energy state of an electron
<i>G</i>	Shear modulus
<i>C</i>	Concentration
2D	Two-dimensional
3D	Three-dimensional
FITC	Fluorescein isothiocyanate
FRAP	Fluorescence Recovery After Photobleaching
FCS	Fluorescence Correlation Spectroscopy
OPT	Optical Projection Tomography
FRET	Förster Resonance Energy Transfer
FLIM	Fluorescence Lifetime Imaging Microscopy
NMR	Nuclear Magnetic Resonance
PFGSE	Pulse Field Gradient Spin Echo

1. INTRODUCTION

Hydrogels are versatile aqueous polymer networks that are used in contact lenses, controlled drug delivery applications and tissue engineering in formation of artificial tissues such as skin and cartilage [1]. Polymer materials are versatile and adaptable, and properties of hydrogels can be modified to form dynamic microenvironment to cell cultures. Hydrogel scaffolds are aimed to mimic the extracellular matrix (ECM) in cell cultures which is present in natural tissue. Since tissue engineering constructs usually lack vascularization, mass transport properties are one of the key perspectives in designing three-dimensional (3D) scaffolds and maintaining viability of the cell culture. Manufacturing scaffolds with sufficient exchange of substances can be obtained with diffusion studies and methods for revealing diffusion behaviour in varying hydrogel materials have been developed.

3D cell cultures are mimicking cellular environment in tissues and are a tool for studying and modelling biological function in cellular, tissue and organ level. 3D cell culturing is complex system in which environmental factors such as pH, temperature and supply of oxygen are adjusted. In development of 3D cell cultures, mass transport is one of the most important parameters to take into consideration as it is necessary to maintain the sufficient change within gases, nutrients and metabolite and waste products. Sufficient mass transport is limited by cell aggregation and therefore local environment can be hypoxic and lack nutrients. Furthermore, environment can be toxic, as loss in exchange of metabolites produces toxic waste products. Increasing porosity of scaffold material can enhance mass transport properties even though the balance between porosity and mechanical strength need to be considered. [2] Therefore, the aim is to modify properties of 3D scaffold to enhance formation of 3D cell culture with required rate of mass transport.

Hydrogels are used in tissue engineering scaffolds to 3D cell cultures and physical, mass transport and biological requirements can be adjusted. Scaffold is designed to compensate the extracellular matrix (ECM) in tissues and sufficient mechanical support for cell culture in tissue models is essential physical parameter to achieve, along with desirable degradation time and process. Additionally, mini-invasive application to the delivery site can be obtained with adjustable gelation process. Mass transport is mainly occurring through diffusion, and therefore optimizing parameters of hydrogels that have effect on diffusion behaviour is essential as transfer of substances is critical for viability of the cell

culture as discussed previously. Requirements of tissue engineering scaffold include biological factors such as biocompatibility and enhancing cellular adhesion, proliferation growth and differentiation. [3, p. 113] In this work, focus is kept on hydrogels' diffusion properties with consideration of parameters that have impact on diffusion behaviour in hydrogels.

The aim of the literature review is to introduce and map the methods that are used to measure diffusion in hydrogels. At first, hydrogels are briefly discussed in general along with explanation of affecting parameters on diffusion in aqueous polymer network. Introduction of basic principles of diffusion in hydrogels is followed by presenting fluorescence-based and other, non-fluorescence methods. Fluorescence methods are used to detect the mobility of a probe molecule with measuring fluorescence intensities and estimating the diffusion coefficient from fluorescence signals. Several fluorescence methods are explained and principles of the techniques are introduced. Calculation of diffusion coefficient can be obtained additionally from Nuclear Magnetic Resonance (NMR) and Raman spectroscopy measurements, and those methods are additionally presented with brief theory background. Summary and discussion of the methods are included in the conclusion chapter.

2. HYDROGELS

Hydrogels as polymer materials are adjustable in chemical and physical properties and utilized with various techniques. Necessary requirements such as sufficient diffusion for biomedical purposes can be obtained by selecting suitable source materials and manufacturing method.

2.1 Hydrogel properties and structure

Hydrogel structure consists of hydrophilic crosslinked polymer chains that form 3D-network [4, p. 146]. There is a growing rate of different hydrogel products, and hydrogels can be classified based on origin and structure as well as chemical, physical and electrical properties [5]. Network can be formed from natural or synthetic polymers and hybrid polymer network contains both, natural and synthetic polymer types. [6, pp. 31–32]. Polymer network is formed from different monomer and macromer components and therefore can be homo- or copolymer [3, p. 107]. In addition, the basis of hydrogels can be natural or synthetic cross-linked polymer combined with another polymer network and those hydrogels are classified as Interpenetrating Polymeric Network (IPN) -hydrogels and are not crosslinked with chemical bonds [7, p. 157].

Hydrogels have differences in concerning cross-links and their electrical properties. Chemical hydrogels are cross-linked with covalent bonds and physical hydrogel's cross-links can be from hydrophobic interactions and hydrogen or ionic bonding [5]. The amount of crosslinking polymer chains is described with hydrogel's cross-linking density (*CLD*) [8]. Electrical properties are classified based on the ionic nature of the chains in crosslinks. Hydrogel can be nonionic, ionic as anionic or cationic, or contain both anionic and cationic groups and classified as Zwitterionic. [4, p. 149] The space between cross-linked polymers can be represented with a mesh size parameter (ξ) which is the length between crosslinked polymer chains [8].

The classification of hydrogels is additionally made between different pore sizes of hydrogels. Hydrogels as hydrophilic porous materials, have free space between polymer network chains and those pores filled with water. Porosity is classified as nonporous, microporous (pore size 10 nm–10 μ m), microporous (pore size >10 μ m) or superporous [6, p. 34,54]. Varying porous structures can be achieved with different manufacturing methods. The amount of porosity, pore shape, size and their connections affect to the bioactivity, mass transport and mechanical features of hydrogels [6, pp. 65–66].

Hydrophilicity of hydrogel material is a key feature, and it causes swelling or shrinking in different circumstances. The level of chains' hydrophilicity and therefore amount of water in the macromolecule network depends on functional groups and that can be adjusted with varying the ratio of hydrophilic and hydrophobic monomers as synthetic polymer being more hydrophobic [5]. Equilibrium swelling ratio (Q) is determined from weight of the swollen hydrogel compared to the dry gel weight [6, p. 155] and swelling ratio (SR) is calculated as ratio of weigh difference in swollen and dry states compared to the dry weight. SR is equal to the water content of hydrogel and depends on hydrogel structure, ionic strength, pH, hydrophobicity and the crosslinking. [8] Finally, increased porosity enhances the swelling process due to the water filling the pore space [6, p. 62] and therefore porosity and swelling affect diffusion behaviour.

Intelligent hydrogels have ability to change the volume based on the environment. Physical and chemical stimuli causes hydrogel to shrink or swell reversibly returning to original shape. [6, p. 7] Changes in temperature, electric or magnetic field, light, pressure and sound are physical stimulation. Chemical stimuli can be change in pH, ionic strength, solvent composition and can be an enzyme for example. [5], [6, p. 150] The swelling of hydrogel, biological contact as an example of stimuli, enables the usage of hydrogels in controlled drug release applications [6, p. 13].

Versatile properties of hydrogels allow the usage in tissue engineering as scaffolds. Depending on the crosslinking state and size of porous structures in nanometre scale, hydrogels offer microenvironment to cells and cell clusters and interconnectivity of clusters [6, p. 12]. In addition to biological advances that enhance cellular functions, differentiation, proliferation and adhesion, physical and mass transport properties can be obtained. Hydrogel synthesis, biodegradation and mechanical criteria are adjusted considering the application. [3, p. 113] As a summary, tailoring requirements for tissue engineering scaffold needs to be considered in physical, chemical and biological perspectives and acknowledge them within the whole lifespan of hydrogel, from manufacturing to the degradation process.

2.2 Hydrogel synthesis

Manufacturing of hydrogels and crosslinking process depends on the usage of natural or synthetic polymers. Polymers, natural polymers included, can be crosslinked with chemical reaction, radiation or formation of physical interactions depending whether the

hydrogel is physical or chemical hydrogel [5]. Figure 1 illustrates the differences in physical and chemical structure and gelation mechanisms. Synthetic hydrogels are manufactured using separate initiator or irradiation with monomers and crosslinkers. Initiators can be radicals such as benzoyl peroxide or ammonium peroxydisulphate that directly or indirectly crosslink the chains to each other. [6, pp. 147–148] Irradiation method can include gamma rays, electron beams [5], UV rays or microwaves [6, pp. 147–148] as initiator. Additionally, polymerization process can be bulk, solution, suspension, or inverse suspension polymerization and hydrogels are produced as form of matrix, film or microsphere [5] depending on the used polymerization method.

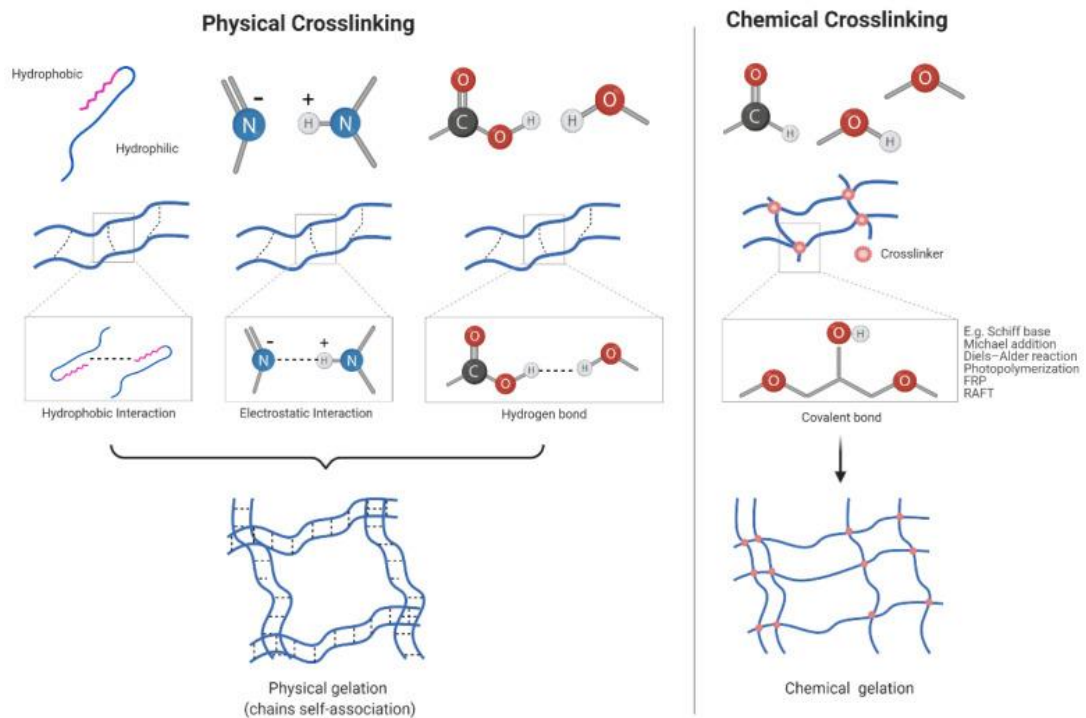


Figure 1: Physical and chemical hydrogel's gelation mechanisms and structure. [9]

Formation of hydrogel scaffolds for medical purposes can be done with many techniques and there are structural demands such as optimized porosity, pore size, pore interconnectivity and geometry combined with mechanical properties [4, p. 154]. The fabrication method can be chosen in a way that it has beneficial impacts on hydrogel's diffusion properties. For example, transport can be enhanced with fiber mesh technique [4, p. 152,154]. Additionally, crosslinker's properties affect to the structural parameter, mesh size and selecting crosslinker with higher molecular weight can increase the rate of diffusion [10] and therefore tailoring diffusion properties with fabrication techniques can be done in different structural levels.

Deciding the fabrication method for a cell culture scaffold needs consideration of biocompatibility and toxicity. After polymerization, possible residues from initiators, monomers, oligomers, crosslinking agents and possible side reaction products are removed [5]. Residual monomers can be toxic and leaks of monomers from hydrogel can occur [6, p. 147]. Particulate leaching method uses compounds such as salt to produce a porous structure and there might be residues of pore-making molecules or other solvents [4, pp. 150–154]. Diverse polymer scaffold manufacturing methods have been developed and therefore requirements in biological properties for hydrogels in medical applications could be reached.

2.3 Diffusion in hydrogels

Mass transport through membrane occurs due to the gradient in pressure, concentration, temperature and electrical potential in different sides of the material [11, p. 21]. Mass transfer depends on the gradient as driving force and described with mass transfer coefficient. Mass transfer coefficient is affected by characteristics of both the mobile molecules and the material as membrane. [11, pp. 32–33] In this work, molecular diffusion and concentration gradient as mass transport force, are used as mass transport mechanism and mass transfer therefore considered with diffusion coefficient which is used to demonstrate the diffusivity of fluxing molecules in the material.

Molecular diffusion can be modelled with Fick's first law in which transfer rate, the flux (J) is written as

$$J = -D_{AB} \frac{dC}{dy}, \quad (1)$$

and it is directly proportional to the diffusion coefficient (D_{AB}) of the molecule A flux in solute B and depends on the concentration (C) gradient of A in direction (y). Molecular diffusion in hydrogels is characterized with diffusion coefficient and can be in scale of 10^{-5} cm²/s to 10^{-8} cm²/s [12].

Permeability, the molecules' ability to permeate the hydrogel membrane, can be measured and calculated with permeability (P_i) of a diffusive molecule. The value of permeability can be determined from multiplication of partition coefficient (K_i), which is the ratio between solute concentrations in the gel membrane and in the solution, and solute's diffusion coefficient (D_i) as follows

$$P_i = K_i D_i. \quad (2)$$

Permeability depends on both thermodynamic and diffusion properties of the diffusive molecule and can be used in estimation of diffusion properties of hydrogel. [12]

Diffusion can be modelled with calculated probabilities of the molecule movement through the hydrogel polymer network and in hydrogels, the diffusion mainly occurs via water that is surrounding the polymer chains. The polymer network of a hydrogel has free space between polymer chains and free volume theory is used to estimate the probability of a molecule to find free pathway. Additionally, obstruction theory can be used to model molecular diffusion. Polymer chains of hydrogel network act as barrier and change the direction of solute and diffusion is characterized with probability of passing polymer chain. The two models estimate the diffusion in consideration of hydrodynamic radius of fluxing molecule and molecular weight and mesh size of hydrogel. [13]

In hydrodynamic theory, diffusion is affected by the aggregation of diffusive molecules in the polymer network due to polymer-solvent interactions in their interface [14]. Therefore, diffusion coefficient of a molecule A is affected by its effective hydrodynamic radius (r_s) which is the spherical radius of the molecule, and viscosity (η) of the solute B. Stokes-Einstein equation diffusion coefficient can be calculated with equation

$$D_{AB} = \frac{kT}{6\pi r_s \eta}, \quad (3)$$

in which k is Boltzmann's constant, η viscosity of solute and T temperature. [11, p. 70,72]

Molecular diffusion in gel network is affected by the properties of diffusive molecules and larger molecular weight decreases the diffusion coefficient in hydrogel [14], [15]. Additionally, hydrogel bonding and hydrophobic interactions between fluxing molecule and polymer network restrict the diffusion. When hydrodynamic interactions are considered, polymer network restrains solute flow-movement and that decreases the diffusion coefficient. A diffusive molecule with small hydrodynamic ratio compared to the mesh size of the hydrogel, diffuses higher rate than the hydrodynamic ratio being in the same scale with mesh size or even larger. [14] The figure 2 illustrates these affecting factors in the polymer network.

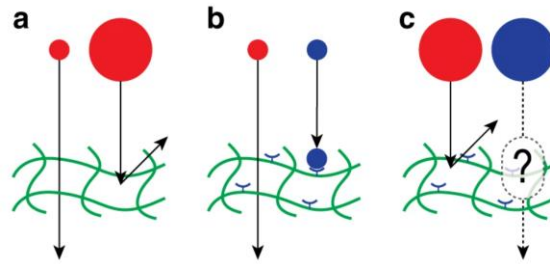


Figure 2: Molecular diffusion in gel network depends on (a) hydrodynamic radius and therefore the size and (b) intermolecular interactions. (c) Diffusion of relatively large molecule compared to the mesh size, could require consideration of change in the polymer structure to transport the molecule as movement is restricted in the polymer network. [16]

In addition to diffusive solute properties, hydrogel network properties such as polymer chains, crosslinking density, mesh size and swelling degree have impact on diffusivity. Polymer chain's ability to move in the structure and possible functional groups that attract the diffusive molecules, affect to the diffusion of molecules [13]. Crosslinking density arises from characteristics of used polymer chains and increasing *CLD* decreases the mesh size and swelling ratio and therefore restricts the diffusion [8]. Finally, enhanced porosity can be used to increase the ratio of swelling and the pore structure and properties of polymer chains are considered in optimizing diffusion behaviour.

The basic principles and affecting factors of diffusion in hydrogels have been considered and introduction to the methods to measure and determine diffusion coefficient is presented in further chapters.

3. FLUORESCENCE-BASED METHODS

Fluorescence is a form of photoluminescence along with phosphorescence and the phenomenon is based on the conservation of energy and the fluorescent material's nature to absorb and emit energy of light. An electron of a fluorescent material has a normal state of energy (S_0) and due to the absorption of a photon, the electron is lifted to the upper level of energy. After the full excitation, non-radiative transitions occur as heat released by vibrational relaxation and electron falls to the lowest excited state (S_1). Emission of fluorescent light can be seen in radiative transitions when the excitation discharges and electron's energy decreases towards to the ground state. There can be additional non-radiative transitions between reaching the ground state and the figure 3 illustrates the fluorescence cycle. [17], [18, pp. 86–90]

Material's excitation and emission spectre is defined by the absorbed light's wavelength with molecule-dependent energy loss in vibrational relaxations [13]. The fluorescence peak in the emission stage has a transition compared to the peak of excitation and that is referred as Stokes shift. The transition is caused by non-radiative decreases in energy states of the fluorescence molecule and causing emission wavelength to be longer and in lower energy. [18, p. 88] Dependence of fluorescence excitation and emission to the wavelength is shown in the figure 3.

Fluorophore is a compound that has ability to produce fluorescent light and they are used as labels. Molecules that are targeted, can be modified with organic fluorescent dyes or genetically encoded fluorescent proteins. As mentioned earlier, fluorescent molecule has characteristic ability to produce fluorescent signal and in addition to excitation and emission, fluorophores vary in fluorescent lifetime. [18, pp. 133–136] In diffusion studies, fluorescein isothiocyanate-dextran (FITC-dextran) are common chemically conjugated fluorophores to dextran polysaccharides and they are used in various molecular weights. FITC-dextran in different sizes can be modelling diffusion of necessary compounds that are needed in hydrogel cell cultures such as glucose, proteins, proteoglycans and waste molecules [19].

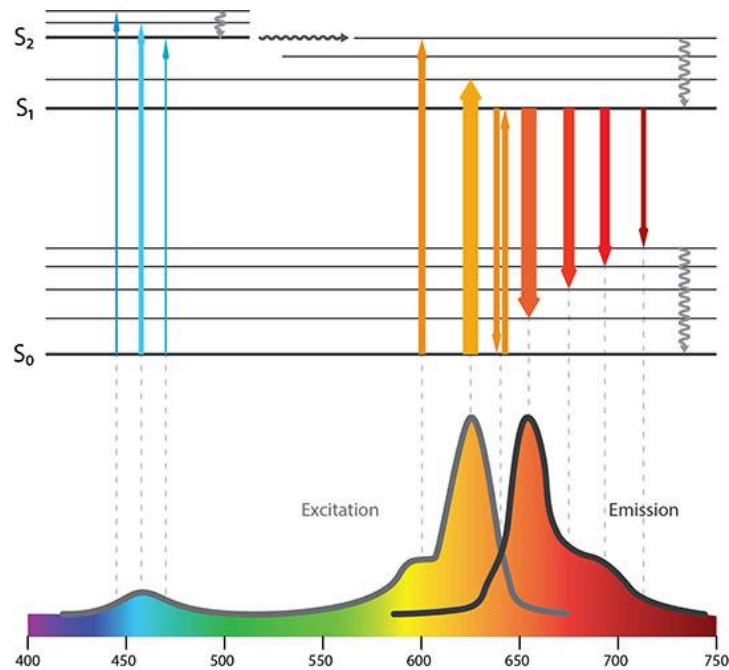


Figure 3: Excitation and emission of a molecule correlates to its fluorescence spectra as energy level (S) in radial axis and wavelength of light in horizontal axis. The second diagram illustrates the probability for excitation and emission in different wavelengths. [17]

Fluorescence is conventionally measured with confocal microscopy as fluorescence spectroscopy method. In confocal microscopy, laser beam is guided to the sample from light source and emission of a fluorescent light measured with detector. The main principle is that all light that is emitted from the focus area, is directed through lens and pinhole to the detector. By changing the depth in which the sample is measured, two-dimensional (2D) optical information can be detected and 3D-illustration of a sample can be reconstructed. [18, pp. 166–169]

In detecting fluorescent light with microscopy, different wavelengths of light are separated with filters and dichroic mirror. Excitation and emission filters are determined to reach the fluorescent spectre of a molecule that is used, and Stokes shift transition acknowledged in selecting the filter. Wavelength of excitation is chosen considering the phototoxic effects along with reducing the autofluorescence of the biological sample. Additionally, unintentional photobleaching which is determined as fluorochromes loss in fluorescent function due to high-power light can be avoided with selecting the suitable excitation light. The dichroic mirror reflects the excitation light from the light source and transmits the emission light to the detector. [18, pp. 98, 134–136] Schematic array is represented in the figure 4 and it illustrates basic elements of fluorescence detecting setup.

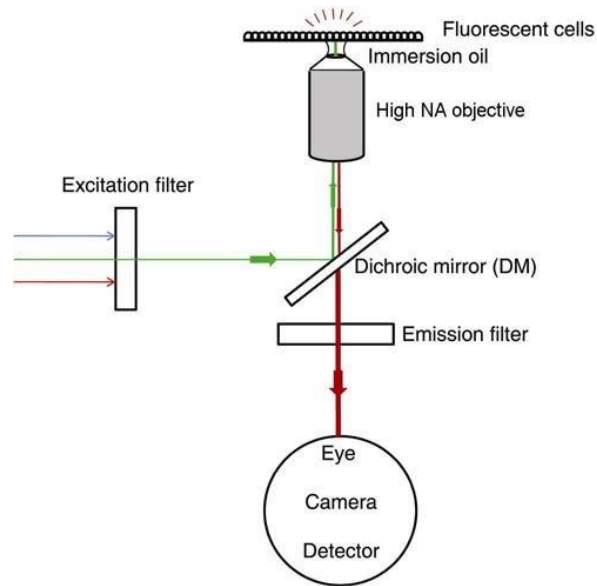


Figure 4: Schematic illustration of the fluorescent detecting array with excitation and emission filters in the fluorescence microscope. [20]

Fluorescence microscopy can be utilized in diffusion studies with tracking the diffusive molecule's mobility and localization. Furthermore, fluorescent sensors enable estimating diffusion properties in hydrogels with measuring quantity of diffusive molecule in hydrogel structure. These fluorescence methods are discussed further in the following chapters.

3.1 Detecting mobility of fluorescein molecule

Several fluorescence methods have been applied to diffusion characterization of hydrogels and tracking the movements of fluorescein probe with measuring fluorescence intensity is used to calculate diffusion coefficient. Fluorescence microscopy approaches can be used, and their ground principles are introduced with experimental studies.

3.1.1 Mobility in capillary hydrogels

Hettiaratchi et al. introduced a method to measure diffusion coefficient with tracking fluorescent proteins in hydrogels manufactured as capillary tubes. The diffusion coefficient was determined from diffusion from bulk solution with theoretical model and experimental arrangement and that is illustrated in the figure 5. Fluorescence intensity of diffusive proteins in different molecular weights such as bone morphogenetic protein-2 (BMP-2) was detected with inverted laboratory microscope as intervals of 4 minutes for 2 hours. The researchers used two natural-derived hydrogels with different mass concentrations: 2% (w/v) alginate and 6% (w/v) collagen and additionally synthetic cross-linked hydrogel, 4% (w/v) poly(ethylene glycol) (PEG-MAL) and the size of capillary tubes was 100 mm in

length and 600 μm in diameter. The method was showed to be efficient when considering the low consumption of fluorescence label and observing time of the diffusion. Accuracy of the method could be applicable in optimizing hydrogel's diffusion properties. [21]

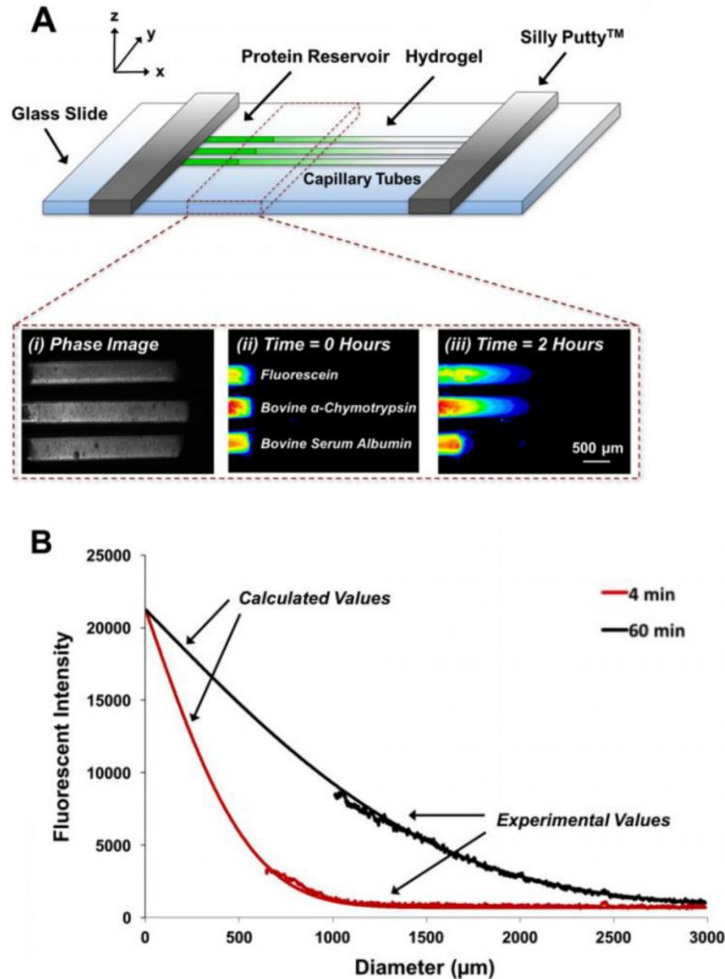


Figure 5: (A) Research arrangement of diffusion coefficient measurements in capillary hydrogels and (B) the correlation between theoretical and experimental results. Fluorescent intensity of a protein and diameter of tube are considered with the measurement time. [21]

Diffusion coefficient in synthetic hydrogel, PEG-MAL was found to be lower in all researched proteins compared to alginate and collagen hydrogels. Additionally, diffusion coefficient was larger in proteins with smaller molecular weight as expected. The mathematical model is based on the one-dimensional diffusion, and it was found that the experimental results followed the model even though the determined diffusion coefficients were higher compared to literature overall. Higher values of diffusion coefficients can depend on the setup. Polymer concentration, crosslinking density, concentration gradient and geometry of the research arrangements varies between different set-ups and that effects on the comparison of the results. Diffusion was guided through an empty

hydrogel network from a relatively large path of solution and there might have been other forces than concentration gradient. Protein aggregation depends on hydrodynamic radius of a protein and high concentrations and literature values might have been lowered by the phenomenon. [21] The efficient method offered possibility to measure many samples simultaneously in large imaging area and therefore sample size is not restricted.

3.1.2 Fluorescence recovery after photobleaching

Fluorescence Recovery After Photobleaching (FRAP) is a method based on the generated loss to the molecule's ability to emit a fluorescence signal, defined as photobleaching. High intensity light is used to generate fluorochrome destruction or create covalent modifications that restrain the fluorescence in the region of interest (ROI), which is the detection area of mobility measurements. After photobleaching, the recovery of fluorescence in ROI is detected. The recovery process can be used to understand the diffusion of molecules and compartments' movements through the sample. Due to the loss in amount of fluorochromes in ROI, total intensity of fluorescence decreases in the researched sample. FRAP can be used to target molecular diffusion, intracellular movements and interactions and molecular binding to proteins and structures. Additionally, immobilization of different compartments in the material can be studied. [22] Figure 6 illustrates the principle of FRAP and intensity curve of fluorescence after photobleaching.

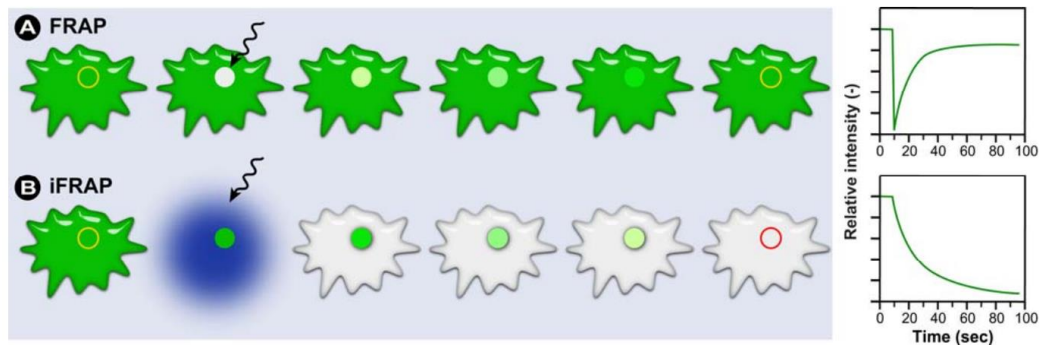


Figure 6: The basic mechanism of fluorescence photobleaching and recovery in FRAP and in inverse FRAP (iFRAP). The area around the ROI is photobleached in iFRAP and it is used in studying smaller ROIs. [22]

The protein mobility can be understood from the detected fluorescent intensity curves. After the photobleaching, the basic intensity of fluorescence (I_i) falls to the lowest value (I_0) and during the recovery process intensity raises to the highest recovery level, referred as maximal plateau value (I_∞). Diffusion properties can be determined from the recovery curve with mobile fraction (M_f), which is the intensity between the lowest intensity after photobleaching and maximal plateau value (I_∞). Recovered intensity at maximal plateau

value is lower than pre-bleaching intensity and the difference is determined as immobile fraction (IM_f). The value of immobile fraction can be used to understand the rate of movement of molecules in ROI. Mobility is classified within three description based on FRAP recovery curve: highly mobile which is not affected by immobile fraction, intermediate with immobility fraction and immobile without significant recovery. [22] The mobility classification along with basic principle of FRAP-curve is illustrated in the figure 7.

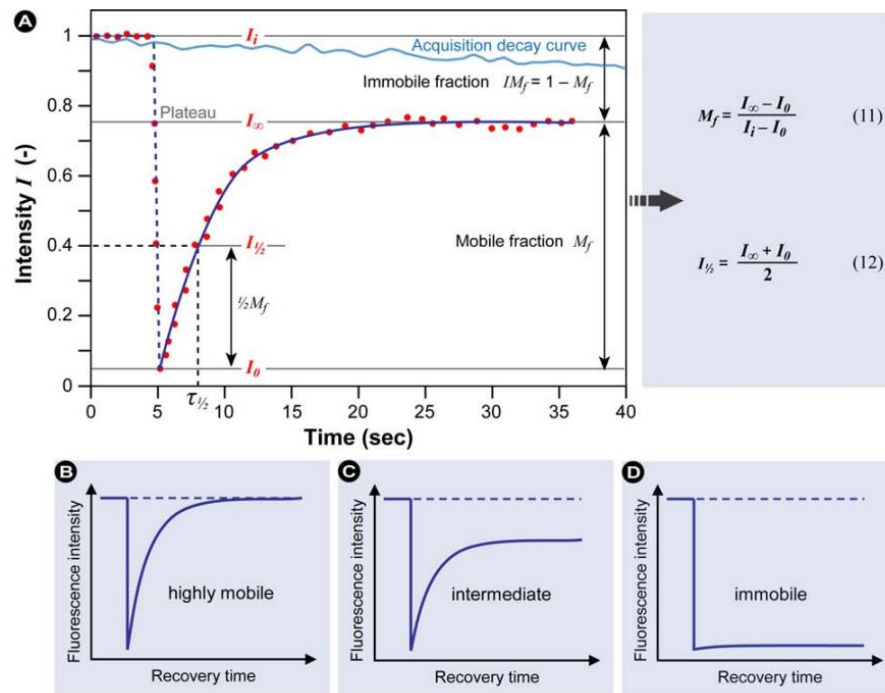


Figure 7: (A) FRAP intensity curve illustrates the fall of fluorescence after photobleaching and the recovery process with equations of mobile fraction (M_f) and intensity in half of the mobile fraction ($I_{1/2}$). Immobile fraction (IM_f) is determined as the difference between pre-bleach intensity and the plateau value (I_∞). Rate of mobility of the researched molecule can be estimated from fluorescence intensity recovery time curve and described as (B) highly mobile without immobile fraction, (C) intermediate and (D) immobile. [22]

Richbourg and Peppas studied diffusion of three fluorescent molecules in hydrogels with FRAP and measurements were analysed with high-throughput method. Diffusion behaviour was studied considering size of the diffusive solute and hydrogel polymerization rate, polymer volume fraction and mesh properties. Solute immobilization in the hydrogel network considering solute size and type and hydrogel mesh size and its correspondence to diffusivity was researched. Diffusion of fluorescein, three sizes of FITC-dextran and FITC-poly(ethylene glycol) (FITC-PEG) from bulk solution to 18 variant hydrogels in the size of 5 mm diameter and approximately 2 mm in height was measured. Photobleaching was created with high-intensity laser and a confocal microscope to image the fluores-

cence. The more efficient automatic analysis method was found to be reliable in comparison to manual data-analysis which was performed parallel with the high-throughput version. [23]

Diffusivity and hydrodynamic radius of a fluorescent molecule was measured as fluorescein having smallest solute size and therefore highest diffusion coefficients. FITC-dextran with increased solute size compared to fluorescein expressed lower diffusivity but FITC-PEG had increased diffusivity with increasing hydrodynamic radius. All three fluorescents showed enhanced diffusion with larger mesh radius which interprets the estimated radius of a solute that can diffuse through hydrogel network. Immobilization of a solute in hydrogel network was calculated and it was found that polymer volume fraction affects to the immobilization in addition to the mesh radius. FITC-dextran showed higher immobilization and therefore lower diffusion rate with increasing solute size. Controversially, immobilization in FITC-PEG was found in smaller size in low polymer volume fraction. [23] Figure 8 illustrates these results from FRAP measurements.

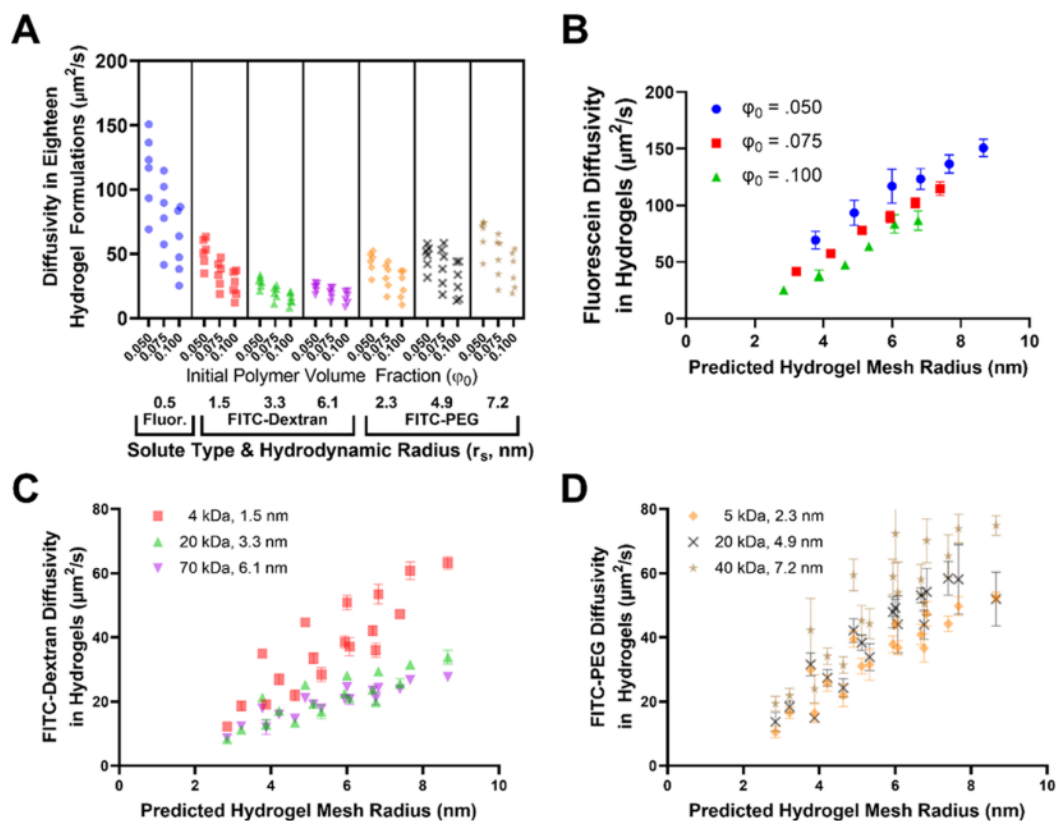


Figure 8: (A) Diffusivity of three fluorescent molecules considered with initial polymer volume fraction of hydrogel. Diffusion coefficients' dependence on mesh radius of the hydrogel for (B) fluorescein, (C) FITC-dextran and (D) FITC-PEG. [23]

Avendano et al. introduced a combinatory method that evaluates structural and mechanical properties with transport characterization of modified collagen I hydrogel matrix. Human recombinant tissue transglutaminase II (hrTGII) and hyaluronic acid (HA) was added to collagen hydrogels in concentrations of 3 mg/ml and 6 mg/ml and the impacts of additives on mechanical, structural and transport parameters were examined and set-up for the study is represented in the figure 9. HrTGII was used as enzymatic crosslinker. Mass transport properties were examined with hydraulic permeability testing and FRAP-imaging using fluorescent trace dyed tetramethylrhodamine isothiocyanate bovine serum albumin (BSA-TRITC) in microfluidic devices. Diffusivity testing was done in hydrogel microchannels with 20 mm length, 3 mm width and 20 μm thickness. FRAP-imaging was used in examining the ROI in the size of 40 μm and diffusion coefficient calculated from the half-recovery time as illustrated in the figure 10. [24]

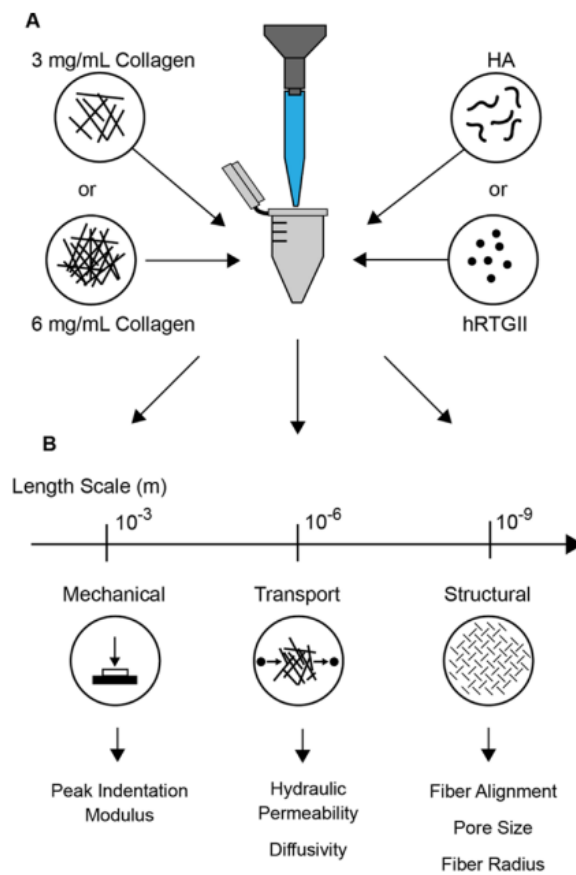


Figure 9: Avendano et al. combined mechanical, mass transport and structural studies to characterize collagen I hydrogels and researched impacts of additives: HA and hrTGII on those properties. [24]

Hydraulic permeability was determined with pressure gradient directed to hydrogel rectangular microchannel with 5 mm length, 500 μm width and 1mm height and movement of BSA-TRITC detected with microscope. Compressive testing was used to examine me-

chanical strength and microstructural characterization with confocal reflectance microscopy, in which the reflection from the sample is additionally collected to form the visualization of the structure, offered knowledge on collagen fiber radius and alignments. Pore size was determined with the nearest obstacle distance (NOD) method and results were used to estimate average pore radius. [24]

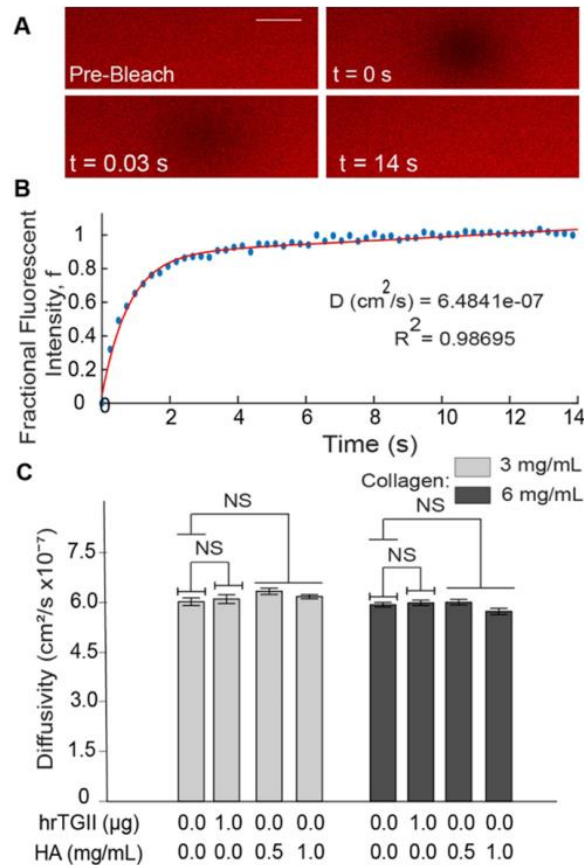


Figure 10: (A) Illustration of ROI and its recovery process, (B) fluorescence intensity recovery curve of ROI and (C) calculated diffusion coefficients from FRAP measurements of hydrogels in two densities and with consideration of the effect of additives (hrTGII and HA). [24]

Addition of hrTGII modified the matrix structure and enhanced the hydraulic permeability whereas HA did not have effect on transport properties and impacted mainly on mechanical and structural characteristics. Because BSA having smaller hydrodynamic radius compared to pore size of the hydrogel, the modified hydrogel structure and densities were not found to have impact on diffusivity although additives changed the fiber and pore properties. Diffusivity FRAP measurements were compared to literature values and theoretically calculated value and those found to correlate. Based on the article, HA in vitro studies reduces the hydraulic permeability because of cell-mediated altering to the localization and distribution of HA in the hydrogel network. [24]

FRAP-imaging was additionally used as a combination with rheological studies to characterize mechanical, rheological, structural and diffusion properties of hydrazone cross-linked hydrogels. Karvinen et al. estimated elastic and viscous behaviour of poly(vinyl alcohol) (PVA) -based hyaluronan (HA-PVA), alginate (AL-PVA) and hyaluronan (HA)-based gellan gum (GG-HA) and hyaluronan (HA-HA) hydrogels. Rheological studies were used to estimate elasticity and viscous behaviour and mesh size, crosslinking density and average molecular weight of hydrogel was calculated. Diffusion of FITC-dextran in four different molecular weights (20, 150, 500 or 2000 kDa) and hydrodynamic radius was traced in the hydrogel sample in volume of 200 μ l. FRAP-imaging was performed with confocal laser scanning microscope and FITC-dextran molecules added during the gelation to the hydrogel. Half maximum was determined from the fluorescence intensity recovery curve and recovery modelled with Virtual Cell software to fit the measured fluorescent data. [25]

FRAP recovery was found to be higher in smaller dextran molecules and diffusion coefficient reaching water's value but larger molecular weights showed decreased recovery. Diffusion might have been affected by heterogeneity of hydrogel structure and therefore be restrained. Additionally, polymer chain mobility and opening can alter the diffusion. Research provided microstructural information combined with rheological and diffusion studies and they were found to be correlating. [25]

3.1.3 Fluorescence correlation spectroscopy

Fluorescence correlation spectroscopy (FCS) was originally developed in late 1900s and can be used to examine molecular movements and interactions by detecting the fluctuation of fluorescent molecules. Fluorescence fluctuations can be measured in femtoliter-scale (fl) in molecular level with 3D confocal microscopy and fluorescent data is further analysed with correlation calculation to determine the causes of fluctuations. [18, pp. 186–188], [26] FCS measurement array is represented in the figure 11.

Correlation analysis separates locations from emitted photons and duration of the fluorescent signal from the same molecule and location. Within the timescale, photons emitted from same molecules are correlated and their movement through the confocal volume of the microscope can be detected. Autocorrelation function is formed from combination of similar signals captured in different points of time. The time between the first detected signal in certain intensity compared to the second signal is referred as time delay (τ). Fluorescence signals that have same intensity are collected and correlation is

decreasing as time delay is increasing. [18, pp. 187–189] Fluorescent molecule's diffusion time (τ_D) is the average time of molecule moving through the confocal volume. Diffusion coefficient (D) of a fluorescent molecule can be determined based on the Einstein's equation

$$D = \frac{w_{xy}^2}{4\tau_D}, \quad (4)$$

in which the w_{xy} is the width of the confocal volume. [26]

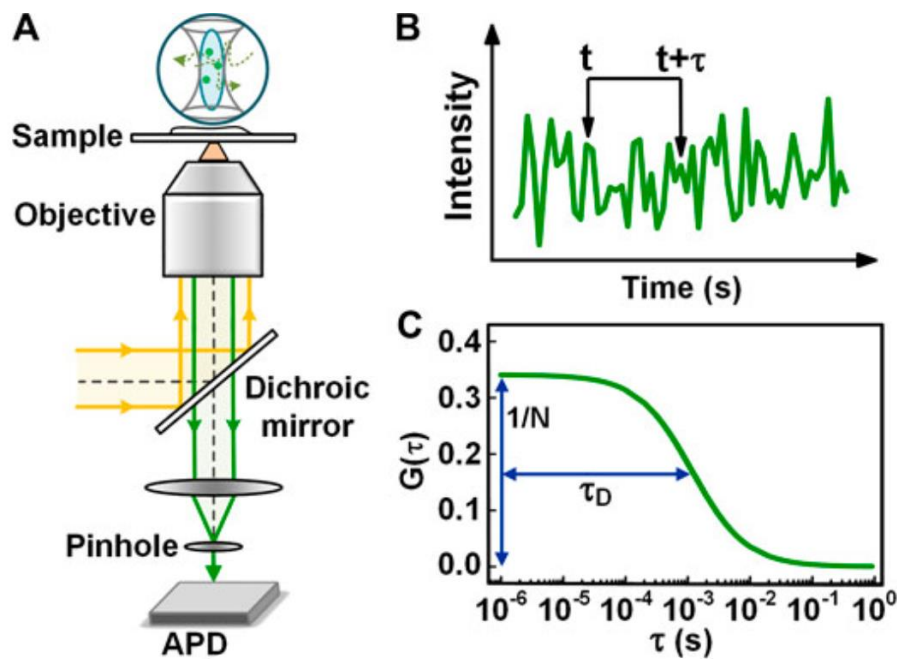


Figure 11: (A) FCS set-up with confocal microscope with (B) an illustration of the FCS -signal of fluctuations in detection volume and (C) a schematic curve of autocorrelation as intensity (G) with time delay(τ) from the fluctuation results. τ_D is the diffusion time. [27]

Zustiak et al. measured protein diffusivity in poly(ethylene glycol) (PEG) hydrogels and results were validated with bulk diffusion studies. Effects of solute hydrodynamic radius and density, mesh size and swelling of hydrogel on diffusion was discussed. FCS was used to estimate the crosslinking, swelling dynamics, solute-hydrogel interactions. Free volume theory from Peppas and Reinhart was applied to diffusivity (D_e/D_0) and measured values are given as ratio of effective diffusion coefficient (D_e) and effective diffusivity in water (D_0). Diffusion of Rhodamine 6G (R6G), enhanced green fluorescent protein (EGFP), bovine serum albumin (BSA) and γ -globulin (Ig) was estimated in three densities (w/v): 5%, 10% and 15% of PEG-hydrogels. In bulk diffusion studies, diffusion coefficient for BSA was calculated with measured release of proteins from hydrogels as

content analysis of solution in which hydrogel was placed and results compared to the results from FCS as illustrated in the figure 12. [28]

Diffusivity of protein was decreased in the increase of solute hydrodynamic radius and polymer density. Swelling ratio decreases as polymer density increases and additionally it was shown that diffusivity was enhanced as swelling proceeded until the equilibrium swelling state was achieved. It was found that in high concentrations of BSA, interactions between PEG and BSA occurred and caused lowered diffusivity even though PEG are thought to be rather inert. Measurements of FCS and bulk solution studies showed correspondence, and FCS offered information about interactions within diffusive proteins and hydrogel. Mesh size was calculated considering hydrogel as homogenous matrix and used solute size that is considerably smaller than mesh radius, but physical entanglement and protein aggregation could have had reduction impact on solute diffusion. [28]

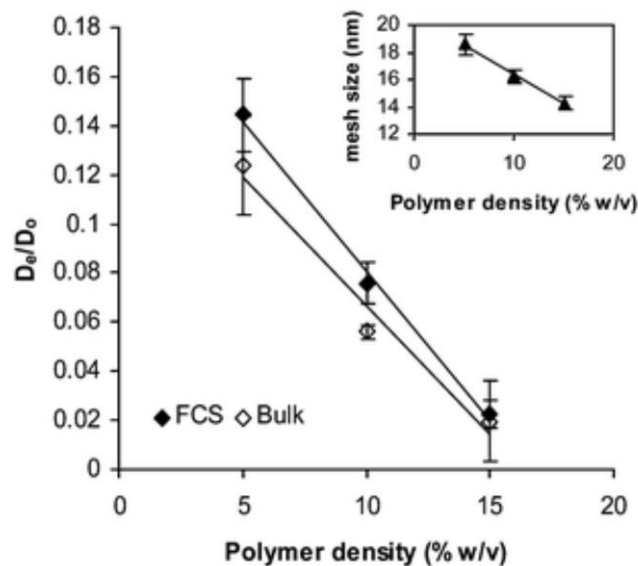


Figure 12: Dependence mesh size (nm) on polymer density (% w/v) of hydrogel in the upper graph and effect of polymer density on diffusivity (D_e/D_0) determined with FCS and bulk diffusion method. [28]

Another study of FCS in diffusion characterization is introduced by Zhang et al. with considerations of electrochemical charge. PEG or dextran solutions in different molecular weights (15-500 kDa) were mixed with fluorescent probe molecules and effect of charge on diffusion in PEG hydrogel studied with positively charged diethylaminoethyl-dextran (DEAE) and negatively charged carboxymethyl-dextran (CM-dextran). FCS imaging was repeated 20 times and measured in time range of 30 seconds. Fluorescent probes' diffusion coefficients were estimated from uncharged PEG solutions in varying polymer concentrations of 1, 3 and 5 wt-%. Diffusion of Alexa Fluor488 (A488) was studied in charged dextran solutions as Alexa488 being negatively charged naturally in neutral pH.

Diffusivity was modelled with Brownian simulation (BD) with considerations of attraction between negative probe and positive polymer environment and rejection force via repulsion of negative probe and negative polymer environment.

Results show that negative probe in positively charged dextran causes reducing effect on Alexa488 diffusion in the gel as expected. Additionally, it was found that the diffusion behaviour of negatively charged A488 in negative dextrans was similar and repulsive interactions to slow the rate of diffusion was not obtained. An agreement with BD simulations and experimental results of diffusion rate being decreased with attraction interactions was found, although hydrophobic and hydrodynamic interactions were not considered in the model. [29]

FCS has been improved with usage of correlation to produce super-resolution knowledge of solute movement in porous material. Kisley et al. introduced a method which combines FCS and Super-resolution optical fluctuation (SOFI) technologies to reveal from particle tracing structural parameters such as pore size and estimate diffusion coefficient. With fluorescence correlation spectroscopy super-resolution optical fluctuation imaging (fcs-SOFI), diffusion coefficients are determined in every pixel from FCS autocorrelation analysis. Pixel intensities which is the data about brightness in each pixel, are collected. Fusing the information from calculated diffusion coefficients in pixels and pixel intensities, the super-resolution colormap of diffusion properties can be obtained from the sample. Colormap is based on the hue saturation value (HSV) in which the hue is normalized logarithmic value of diffusion coefficient. Diffusion in the pores can be determined in nanoscale and pore size evaluated from the amplitude of the FCS correlation curve. [30]

Kisley et al. studied diffusion of N,N'-Bis(tridecyl)perylene-3,4,9,10-tetracarboxylic diimide (DTPDI), which is a single-molecule fluorochrome in fluidic channels and agarose gel with fcsSOFI. Liquid crystal gels were produced from F127 and C12EO10 for capillaries and water composition was 38.6% and 44.1%. Agarose gel was used in concentration of 1 and 2 w/w-%. Diffusion coefficients were calculated, and spatial diffusion map constructed for samples. Compared to single-particle tracking (SPT) and diffraction limited fluorescence imaging, it was found that fcsSOFI gives more accurate and versatile information from diffusion and pore size. Information from structural and diffusion properties can be obtained simultaneously and showed efficiency in detecting signal from background noise. [30]

Preparation of samples for fcsSOFI measurements is uncomplicated but heavy and expensive computational data processing can be limiting the utilization. This was acknowledged by Yoshida et al. and software was developed to enhance the accessibility and

speed in fitting the experimental result to diffusion model. [31] As stated, fcsSOFI does not occur without limitations but if the cost and efficiency in data analysis would be correlating, the method could be applicable to measure diffusion in other hydrogels. Combinatory knowledge about movements of probe molecule and structure could be beneficial in understanding the diffusion in hydrogels. More research is needed on systematic and efficient utilizing the method in hydrogel diffusion characterization and possibly in cell culture systems.

3.1.4 Optical projection tomography

Optical Projection Tomography (OPT) microscopy method allows optical 3D-imaging of complex structures such as small tissues. In OPT, the light is guided with lenses straight through the rotating sample and rotation allows the imaging in different angles and depths. Light that passes the sample placed in the liquid path is directed to the camera and scanned information is used to create 3D-illustration with algorithms. OPT can be used in transmission or emission mode and the latter alternative is used to obtain detection of fluorescence signals. Transmission mode is used to detect the absorption of light to the sample and therefore used to study the structures and shapes. [32]

In addition to conventional microscopy techniques, OPT have been adapted in estimating diffusion properties of hydrogels. Soto et al. introduced an OPT-method for imaging the microtextural and diffusion characteristics of gellan gum (GG) hydrogels with different crosslinking methods. Mass transport was measured as amount of FITC-dextran in different depths as diffusion progressed. Fluorescence of FITC-dextran in different molecular weights was measured with OPT emission mode in hydrogel samples in volume of 1 ml. OPT was targeted in the middle of the hydrogel and FITC-dextran pipetted on top of GG and diffusion of fluorescein imaged each minute in different projection. Structural studies were obtained with transmission OPT and hydrogel's microstructure was determined with projection images reconstructed to 3D-illustration. [19] Figure 13 presents the schematic setup for OPT-imaging.

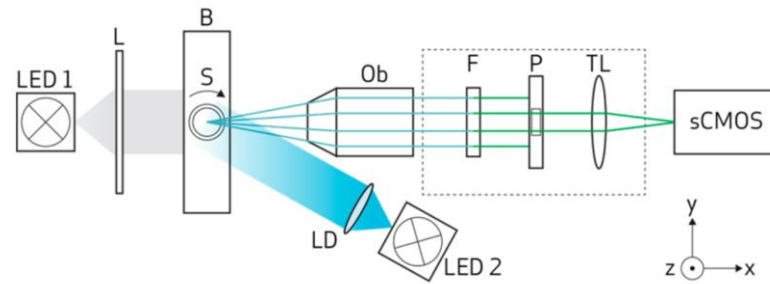


Figure 13: Optical projection tomography measure arrangement which includes lenses (L, Ob, LF and TL), light producers (LED1 and LED2 for fluorescence) to optimize the light observation. The sample is rotating (S) in water batch (B) and light that has passed the sample, is captured by camera (sCMOS). [19]

Structural studies with transmission OPT showed that the method can be used to understand crosslinking density and distribution and additionally the heterogeneity of the hydrogel structure. with time and molecular weight of dextran molecule. The diffusion of FITC-dextran to the hydrogel were considered with depth, time and molecular weight and result showed that in measure times dextrans' with smaller molecular weights diffused deeper. [19] Microstructural properties of GG affect to the mass transport and therefore OPT- imaging is a method for estimate both perspectives. Additionally, OPT- imaging can be utilized in hydrated environment and that is beneficial when studying biological samples.

3.1.5 Förster resonance energy transfer

Förster Resonance Energy Transfer (FRET) is a photophysical process that occurs when two molecules, acceptor and its fluorescent donor are in close distance, at most 10 nm and donor emission and acceptor absorption dipoles in similar angular orientation. Long-distance dipole-dipole-interactions between acceptor and donor results the energy transfer from donor to acceptor without radiation. Both molecule's fluorescence can be measured because energy transfer to the donor molecule accomplishes its fluorescence. In addition to proximity of the molecules, the fluorescence spectres are required to be interwoven with each other in the region between emission of the donor and excitation of the acceptor. [22] Basic mechanism of FRET is presented in the figure 14. FRET-imaging can be used to research individual molecules and their interactions in 3D-cell cultures seeded to hydrogels. The transparency of hydrogel matrix and adjustments in permeability properties can be achieved and therefore hydrogel scaffolds used in FRET-imaging. [33]

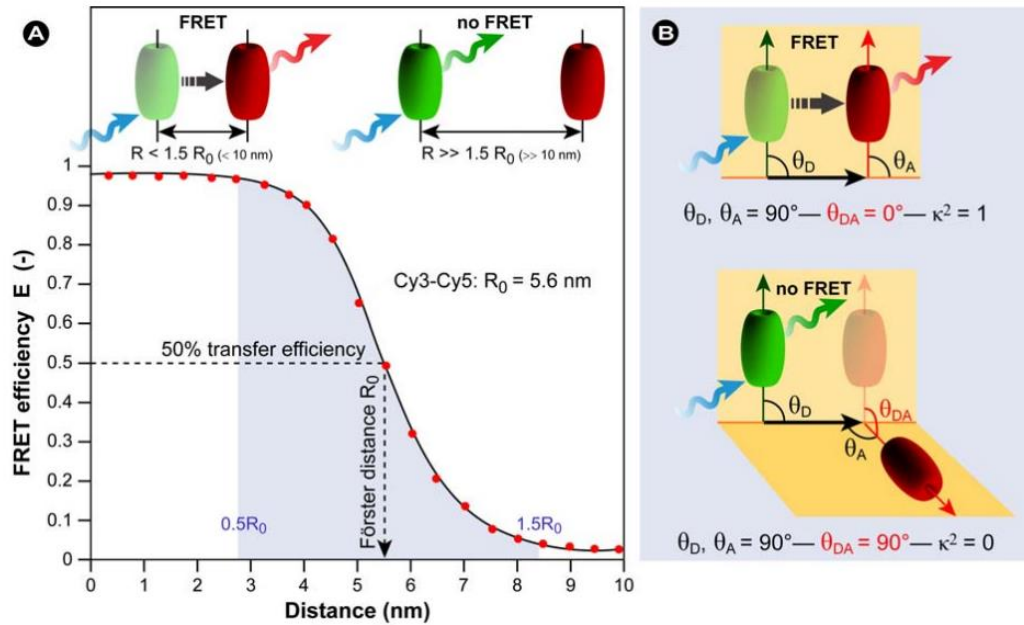


Figure 14: FRET-imaging is based on the FRET-process which occurs when donor and acceptor are in proximity and similar orientation of donor emission dipole moment and acceptor excitation dipole moment. The Förster radius (R_0) is the characteristic distance in half of the maximum FRET efficiency. [22]

FRET-pair was utilized in detection of amount of protein release of cells with sensing hydrogel. Son et al. incorporated FRET-pair in ring-like PEG-hydrogels to measure the diffusion of matrix metalloproteinases (MMPs) from the middle hole to the ring structure. MMPs are enzymes that cleave the proteins with protease activity. Studies were performed with MMP-solutions and MMPs which were secreted by lymphoma cells cultured in the middle of the hydrogel ring. MMPs diffused to hydrogel ring and cleaved constructed peptides that include both FITC and DABCYL of the FRET-pair. Cutting the peptide induced FRET phenomenon between the pair, and fluorescence is measured and concentration of MMPs estimated from increase in fluorescence intensity of sensing hydrogel. Along with experimental studies in protein release, diffusion reaction model was established to simulate the secretion rate and concentration of MMPs. Model showed the concentration profile in the hydrogel ring in different regions and concentration values were calculated from fluorescence increases with time as secretion of MMPs occurred. MMP concentration was found to be estimated in range of 0.6 nM to 40 nM. [34]

Diffusion coefficient was not calculated from the results as Son et al. used the literature value in concentration calculations. As discussed, FRET-imaging can be used in detecting molecular interactions with accuracy of single molecules. FRET-signals give information about the localization of the interaction, and it would be interesting approach to

study transport of a molecule with FRET-imaging as the localization of occurring interactions could be changing during diffusion. Son et al. estimated the concentration of MMPs inside the hydrogel from increase in fluorescence. FRET-imaging might be limited to determine whether the interaction is occurring or not. If rate of interactions in same locations would be observed, the transport of different molecules could therefore be estimated with measuring the fluorescence intensity in different regions of hydrogel with FRET non-invasively. In the previous study, the FRET-sensor for the reaction was incorporated in the polymer network and therefore considerations about impact of FRET pair in biomedical hydrogel would be needed. More comprehensive study and development could be obtained to define the possible role of FRET-imaging in hydrogel characterization.

3.2 Fluorescence sensors

Diffusion properties of hydrogels were evaluated with fluorescence sensors and oxygen and glucose diffusivities determined by Figueiredo et al. Silated-hydroxypropylmethylcellulose (Si-HPMC) – hydrogels were used in varying concentrations, in values of 1, 2, 3.3 and 4 w/v %. Si-HPMC -hydrogel was molded to a cylinder in the size of 1 cm in height and 1.56 cm in diameter for glucose measurements. Glucose sensors were used to detect the concentration inside the hydrogel in 0.5 cm depth and in time range of 50 s as surrounding glucose solution (25 mM) diffused to Si-HPMC. Permeability and diffusion coefficient calculations were accomplished from glucose concentration data gathered with sensors. Si-HPMC in similar size and corresponding positioning of sensor to the hydrogel were used in oxygen studies. Fluorescence oxygen microsensors detected oxygen concentration in two incubation conditions: in hypoxic, in which oxygen content being 5 % and in normoxic as content of oxygen being 20 %. Core pressures of oxygen were measured from incubations firstly in normoxic and secondly in hypoxic environments and calculations of permeability and diffusion coefficient performed from concentration and pressure data. Additionally, studies were performed with in vitro evaluation of cell viability with human adipose derived stem cells (hASCs) in times of 6, 72 and 168 hours with Live and Dead assay and impacts that 3D cell culture has on diffusion of glucose and oxygen estimated. Finally, rheological properties were studied and storage modulus (G') determined and average mesh size calculated. [35]

Glucose and oxygen diffusion was altered by mesh size and reducing mesh size had stronger lowering impact on glucose diffusion. Hydrogel concentration affect to glucose diffusion was not significant whereas oxygen diffusivity decreased with increasing the concentration. The differences in glucose and oxygen diffusivities could be understood because of the chemical properties of them. Oxygen diffusion could be altered because

of the interactions with polymer network. Both glucose and oxygen diffusion are affected by the pore size and geometry of a hydrogel, but it was stated that glucose as water-soluble molecule is affected more by pore parameters. [35]

Cell viability results showed that in higher cell numbers than 4 million/ml when reaching the time of 72 hours, the oxygen level was drastically lowered, and all cells died in the density of 8 million/ml. In densities of 1 and 2 million/ml, viability was high in oxygen measurements. Glucose concentration lowered after 72 hours, in the samples where the cells were seeded with 4 or 8 million/ml densities, but concentration and viability were high in samples of 1 and 2 million/ml even after 168 hours. Based on these findings, oxygen was main reducing factor in the cell culture but additionally, the cell density had impact on glucose concentration. [35]

Sensors have been additionally utilized in other hydrogel applications. Demol et al. used sensors in fibrin hydrogels and mathematical and experimental methods to estimate oxygen diffusion and corresponding cell density in vitro. Effect of oxygen tension on cell growth, viability and distribution was evaluated with human periosteum derived cells (hPDCs) seeded to fibrin hydrogel and oxygen consumption of cells modeled with computational method. Fibrin carrier was used as cylinder in size of 4 mm in height and radius and the cell culture was seeded in density of 10^6 cells/ml after polymerization. Cell density and oxygen tension was modelled in three layers: medium, surface and fibrin carrier hydrogel with cells. Cell viability was analysed in live-dead-assay with fluorescent dye after 0, 7, 14 and 21 days of culturing and cell distribution evaluated at the day 21 with 6-diamidino-2-phenylindole (DAPI) staining and nuclei imaged with fluorescence microscopy. Oxygen diffusion coefficient was measured with setup that consists of two chambers and fibrin hydrogel being placed in between them. The complete system, chambers and fibrin hydrogel is filled with culture medium. The chamber above fibrin hydrogel is aired and oxygen pressure is 21 %. In the lower chamber, nitrogen is used to deoxygenate the space and oxygen microsensor is placed to detect the oxygen tension changes as diffusion through fibrin occurs from upper chamber through hydrogel layers. [36]

Results for diffusion coefficient were calculated from the time range of 0.5 h to 15 h and value of the coefficient was found to be lower than in water. Oxygen tension was decreasing when measured from medium towards the fibrin carrier. In the surface layer, where cell density was highest, amount of oxygen decreased 2.3 % and in hydrogel interiors, oxygen tension falls 16.5 % towards zero and anoxic conditions are formed inside the fibrin carrier. Cell distribution highest in the surface as predicted with the model but cell density was lower inside the hydrogel compared to expectations with mathematical model and degradation might have caused disagreement between experimental and

mathematical results. As studies were utilized in vitro, it was possible to evaluate the oxygen consumption of cells, which affect to the oxygen tension additionally to diffusion properties. Computational model of oxygen consumption agreed with experimental results. Diffusion results were gathered in the gas phase and in liquid environment the diffusion is altered and might be lower. [36]

Computational and mathematic models offered effective tool to model oxygen tension and cell density in hydrogel constructs even though there were some parameters that did not fit to the experimental results such as cell distribution inside the fibrin carrier. Additionally, study offered in vitro oxygen diffusion and consumption studies for 3D cell culture which were mainly noninvasive. Oxygen microsensors were invasive and measured the pressure of oxygen which could limit the understanding of oxygen diffusion. Along with Demol et al, Figueiredo et al. used invasive sensors and diffusivities were determined with measuring local concentrations and therefore reliable estimation of diffusion in the hydrogel material from local measurements could need more studying and consideration on the movements of probe molecule in the hydrogel sample.

4. OTHER METHODS

Non-fluorescent method for characterizing the diffusion properties of hydrogels have been utilized. Raman scattering and nuclear magnetic resonance are additional molecular properties and are exploited in diffusion studies.

4.1 Raman spectroscopy

Raman scattering was observed first in 1928 and Raman spectroscopy is used to image the phenomenon. Raman scattering occurs when a molecule is directed with light and molecule excites higher energy level. In Raman scattering, the excitation is not as complete as in fluorescence spectroscopy and emission of light in Raman scattering is caused by the transitions in vibrational energy levels. Wavelength of Raman scattering depends on molecular properties that interacts with light, not the wavelength of absorbed light as in fluorescence. Therefore, Raman spectroscopy can be used to detect vibrations in different molecular structures such as bonds. The energy difference between the energy states before and after the scattering of light is determined as Raman shift. The energy of emission scattering compared to the excitation light can be in the same level as in Rayleigh scattering, lower as in Stokes Raman scattering or higher as in Anti-Stokes Scattering. Raman spectroscopy results are expressed as light intensity with Raman shift or wavenumber. [37] Different classes of Raman scattering are illustrated in the figure 15.

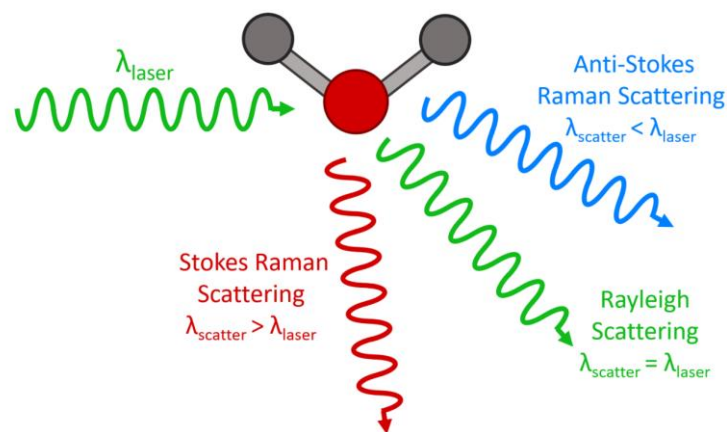


Figure 15: Depending on the scattered wavelength and therefore vibrational energies, Raman scattering can be classified as Anti-Stokes, Stokes and Rayleigh scattering. [38]

Raman spectroscopy can be adapted on diffusion characterization of hydrogels and combined with fluorescence lifetime imaging microscopy (FLIM). Zini et al. introduced a method that can observe Raman scattering of Metronidazole and Vitamin C with complementary metal-oxide-semiconductor (CMOS) single-photon avalanche diode (SPAD) sensor. Rapid laser pulse was used to detect Raman scattering in limited time window and then fluorescence decay was measured in anionic nanofibrillated cellulose (ANFC) hydrogel with three concentrations. Diffusion of a molecule from hydrogel with partially dissolved drug to the area of ANFC not containing drug was detected in two depths. Raman spectroscopy results were given with intensity being the function of wavenumber of scattered light in the diffusion timescale of 5 h to 120 h. FLIM is used to detect the attenuation of fluorescence and therefore characteristic lifetime of molecule to produce fluorescent signal is measured. Vitamin C was measured for fluorescent decay. Fluorescence lifetime analysis was performed in the wavelengths that were lacking Raman scattering. Fluorescence decay was modeled with exponential decay curve fitting and fluorescence intensity formed from summation of intensities in different wavelengths between 1852 and 2022 $1/\text{cm}$. [39] Research setup is presented in the figure 16.

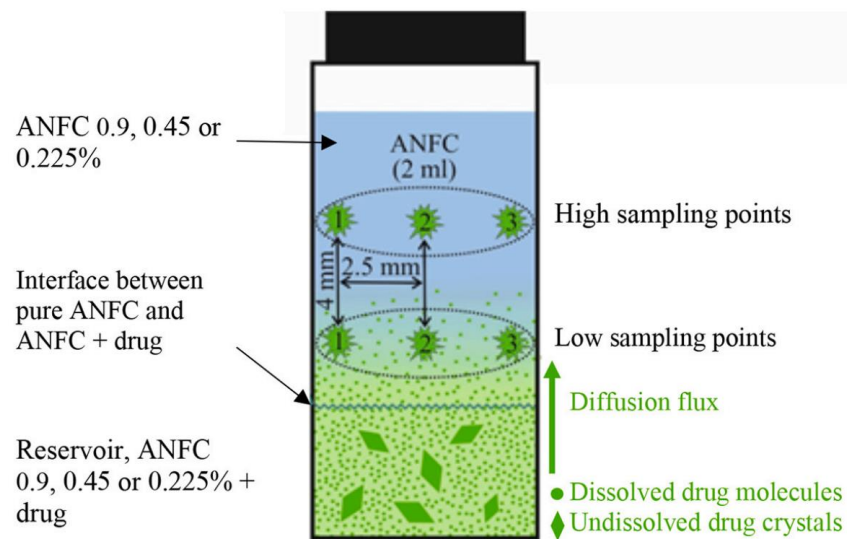


Figure 16: Setup for measuring diffusion coefficient with Raman spectroscopy. Diffusion of drug molecule is occurring from hydrogel (ANFC) with drug to hydrogel without drug. Intensity data of drug molecules is collected from six sampling points in two different depths with Raman sensor. [39]

Diffusion coefficients were calculated from drug concentrations that are estimated from Raman peak amplitudes in different sampling points. Raman and fluorescence radiation were measured simultaneously, and results given as fusion of fluorescence decay with Raman spectra and time. Diffusion of Vitamin C was not significantly altered in different

concentrations of ANFC as Vitamin C being a small hydrophilic drug. Metronidazole diffusion was lower in higher ANFC concentrations. Measured FLIM decay curves were not found to reveal significant interactions with drug and polymer network or degradation as curves were fitting to the calculated exponential decay model. [39]

Diffusivity results were obtained with invasive sensors and that could limit the usefulness of the study even though the measurement was not needing any specific labels and can be utilized in high-water content samples because of the water insensitivity. Raman spectroscopy combined with fluorescence decay offered molecular chemical and physical information about the diffusive molecule and additionally its environment. For example, revealing diffusive molecule's possible binding and degradation during the measurements.

4.2 Nuclear magnetic resonance

Nuclear magnetic resonance (NMR) as a physical phenomenon which describes the ability of nucleus to emit electromagnetic signal when it stimulated with extrinsic magnetic field. Radiofrequency pulse causes protons of nucleus to excitation and therefore rise to higher energy level and that is determined as magnetic resonance. Nucleus consists of protons and neutrons, and those components have magnetic dipole moments, explained as spins. Magnetic dipole moment appears in nuclei that have an odd number of protons and neutrons and therefore the weak magnetic field of the nucleus is possible to form. Random orientation of magnetic dipoles is changed when the external magnetic field is targeted to the sample and direction rotates parallel with the direction of magnetic field due to the torque strength. The relaxation of nucleus occurs as the excitation discharges when external magnetic stimulation is removed, and dipole orientation returns to the original state. Energy emission during the relaxation can be measured with changes in local magnetic fields and that is the detected NMR-signal in NMR-imaging. [40] Figure 17 illustrates the basic principle of nuclear resonance.

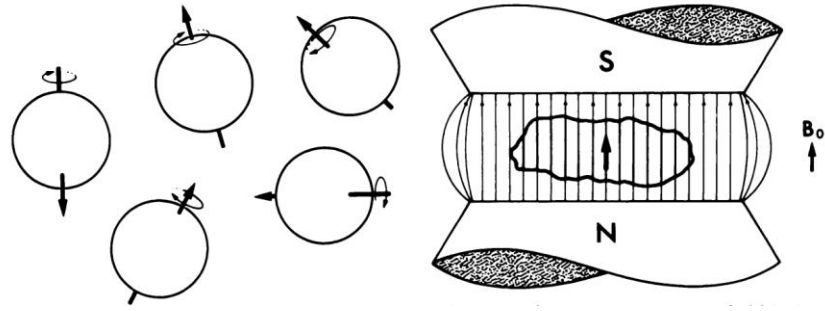


Figure 17: The orientation of nuclear magnetic dipoles changes when external magnetic field is applied. In the first picture, the dipoles are in random orientation (arrows express the direction) without external magnetic field. The second picture illustrates that the orientations rotate to parallel direction with magnetic field as the arrow in the middle of the field and the direction of the field (B_0) express. [40]

Structures and chemical compositions of the material are detected with NMR spectra. Chemical components such as functional groups and bonds have different nature to produce NMR signal due to the different proton and electron cloud and therefore their characteristic resonance frequency matches to the absorbed and emitted energy during the radiative stimulation. The energy difference is called as chemical shift (δ) given in parts per million (ppm) and it represents the change in local magnetic field as the simulation occurs. NMR spectra is formed with comparing the signal peaks in different energy states. [40] Figure 18 presents an example of NMR spectra.

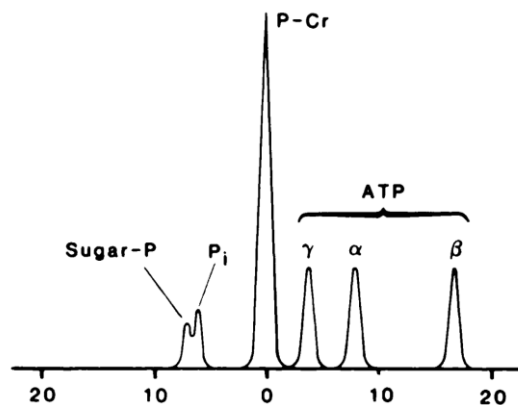


Figure 18: Schematic illustration of the NMR spectra. Chemical shift (δ) is in the horizontal axis and given in unit of parts per million (ppm). NMR peak for sugar-phosphate (Sugar-P), inorganic phosphate (P_i), phosphocreatine (P-Cr) and adenosine triphosphate (ATP) are given as example molecules. [40]

NMR-imaging can be used to study chemical nature of the gel material as well as molecular mobility, solvent diffusion and distribution. Diffusion of molecules can be studied with detecting the attenuation of NMR as the probe molecule is moving further from the targeted radiative stimulation point. Different concentrations, compositions, temperatures and molecular interactions are factors that can be understood with NMR-imaging. Those

results can be obtained based on chemical shift, and differences in spin relaxation times or NMR-signal intensities. Additionally, magnetic resonance imaging (MRI) can be used to detect swelling and polymer chain mobility of hydrogel. [41]

NMR-imaging was used to determine diffusion coefficients of various dextran molecules in polyacrylamide (PAAm) -hydrogels along with fluorescence-based Macroscopic Transmission Imaging (MTI) and FCS as Multiparameter Fluorescence Image Spectroscopy (MFIS) -method. Sandrin et al. determined diffusion in hydrogel after polymerization of PAAm-discs with 0.3 cm radius in MTI and FCS – methods and for NMR-imaging molded as PAAm-cylinder in height of 5 cm and radius of 0.5 cm. Dextran molecules were used as unlabeled for NMR and labelled with Alexa fluor 488 (A488), tetramethylrhodamine (TMR) or fluorescein (FLU) for fluorescence measurements in varying concentrations. PAAm disc was incubated from 2 to 7 days to reach the solution equilibrium in hydrogel and then FCS-imaging was used with confocal detection volume of 0.55 fl and imaged in 18 spots 30 minutes. Hydrogel disc was placed to the dextran solution for MTI and diffusion detected in the time-period of 3 to 72 hours as fluorescence intensity imaged each 5 seconds in the beginning and later in duration of 300 s. Additionally, interactions of small dextrans with polymers were studied in solutions: water, KClO_4 , KCl and potassium carbonate buffer and at pH-level 10. NMR-measurement was performed with diffusion duration of 0.1 to 0.2 s which is the time between pulses and 600-1400 micros long bipolar gradient pulses were used. For NMR-studies, dextran molecules were dissolved to deuterium oxide (D_2O) and water signals from the sample were attenuated. [42]

Dextrans in different size scales were found to correspondent expected rate of diffusion as dextrans with higher molecular weight were determined to have decreasing diffusion coefficient. These results were obtained with all three methods, MNR, MTI and FCS. Information from the methods is gathered in different sizes as FCS is measuring the fluorescence in the confocal volume in spots and MTI was used to image the fluorescence in the whole disc. The impact of accumulation of diffusive solutions with dextrans was minimized during the NMR-studies and therefore lower concentrations used for larger dextran molecules. For MTI-results, dextran concentrations of 0.1 to 10 μM the diffusion coefficients did not vary in that range. FCS-measurements showed interactions between A488-dextran and hydrogel and additionally in MTI-studies, there were higher concentration of the solution inside the PAAm than outside. That indicates that the charge of the dye can affect to the diffusion and that perspective be taken into consideration in diffusion studies. Furthermore, movement and possible interactions within the

dextran molecules and polymer network was modeled and simulations fitted to the experimental results for three methods. [42] The study offered three individual methods for diffusion coefficient estimation and NMR-imaging was found to be comparable to other methods and giving similar information about diffusion in PAAm-hydrogels.

NMR-imaging was applied on diffusion measurements as an individual method. Matsukawa et al. used pulsed field gradient spin echo (PFGSE) -NMR method to determine diffusion coefficients of poly(amidoamine) dendrimer in agar gel and pullulan polysaccharide polymer in gellan gum (GG) hydrogel. During the agar gel formation, before polymerization, the dendrimer solution in concentration of 0.1 wt-% was mixed with agar gel solution. Pullulan solution was added to the GG-solution after swelling and the final amount of pullulan (0.1 wt-%) was reached. NMR spectra was determined in varying temperatures in range of 20 to 60 °C and 1 ms radiofrequency pulse was performed every 10 ms. Rheological parameters, mesh size and diffusion coefficients and their relationships were evaluated in different temperatures as gelation occurred. Gels were utilized in high temperature and cooled 0.5 °C in minute and diffusion and mesh size measuring was continued for 12 days. [14]

Gelation process was detected with NMR, and it was found that diffusion coefficient of dendrimer is decreasing as temperature is decreased. Rapidly cooled agar gel was stored for 10 days, and it was found that diffusivity along with mesh size was increased during the time. The reason to the behavior was stated to be agar molecules in solute form and their interactions with gel network. Viscoelastic parameters were measured with GG with pullulan solution and GG-solution molecules were found to interact with GG network in the same manner as with agar gel. Dendrimer and pullulan did not significantly interact with gelation process, and they were lacking intermolecular interactions with gel network. It was found in the study that additive solute molecules were not interacting straightly with the network and therefore interactions might not be the limiting factor the diffusion. [14] NMR measurements were performed partly in high temperatures and might be limited by the sensitivity to water. The method offers understanding about the impact of temperature on diffusion coefficient and mesh size as well as additive solute role in the gelation process.

Diffusion characterization methods have been introduced in previous chapters and parameters of the gathered methods are represented briefly in appendix A in a form of table. Additionally, shallow discussion of advantages and disadvantages between fluorescent and non-fluorescent methods is offered in the table.

5. CONCLUSIONS

Sufficient availability of necessary substances such as nutrients and oxygen in 3D tissue engineering constructs is one of the required properties. Hydrogels are polymer structures with modified porosity and high water content and exchange of nutrients and waste products is occurring mainly through diffusion. Tailoring the mass transport, biological and physical requirements for 3D cell cultures is a challenge and it has been found that despite of high porosity and water content, diffusion in hydrogels is limited and therefore characterization of mass transport properties of hydrogels is essential when designing and manufacturing hydrogels for 3D tissue constructs. Diffusion coefficient is commonly used value for describing the diffusion properties and it is affected by chemical and physical parameters of hydrogel and diffusive molecule. Established methods for characterization of mass transport properties are still being evaluated and validated and this thesis gathered fluorescence and non-fluorescence method for the purpose.

Hydrogels were briefly introduced and discussed about parameters that constitute the diffusion properties. Characterization methods were described with introduction to the ground principles of fluorescence, NMR and Raman spectroscopy methods. Majority of the methods used fluorescent probe to detect the mobility of molecules and diffusion coefficient was calculated from the results in changes of fluorescence intensity in hydrogel. Fluorescent sensors were used to detect glucose and oxygen and possibility to utilize FRET- sensors in diffusion studies briefly discussed. Fluorescence measurements can be obtained with simple equipment and sample procedures and compared to NMR, microscopy setup be more accessible. Along with diffusion studies, hydrogel structure was characterised and therefore methods that can offer information about both perspectives, such as OPT, could be important method in mass transport studies as diffusion behaviour is affected by both of solute and hydrogel properties. Fluorescence methods are limited to the lacking autofluorescence of diffusive molecules and specific fluorescence dyes are needed and they are used widely. Therefore, NMR and Raman spectroscopy approaches would be decent tools to study without fluorescence as Raman spectra is measured outside the fluorescence energy range and NMR-imaging is obtained with magnetic properties of materials. Additionally, NMR and Raman spectroscopy can give information about chemical structure of a molecule and hydrogel.

Along with experimental arrangements, computational and mathematical models were obtained for diffusion and structure studies. With understanding the theoretical framework of diffusion in hydrogels and as a phenomenon, simulations were used to model

and predict the diffusion behaviour. Additionally, hydrogel's structural properties such as mesh size and crosslinking density were calculated, and impact of those structural parameters used to understand the diffusion measurements. New models and simulations were introduced with comparison between experimental results and computational estimations. Finally, if diffusion behaviour could be reliably predicted with models, it might reduce the costs and increase the efficiency of understanding the impacts of different hydrogel parameters, such as crosslinker and crosslinking density, have on diffusion in hydrogels. Those impacts could be modelled beforehand and valuable information could be used to optimize the samples for experimental studies.

Several approaches to measure fluorescence intensity and detect probe molecule's mobility were introduced. Transport of molecules was studied imaging the fluorescence within the entire sample or depending on the method, in detection area or volume. Following the movements of fluorescent probe molecule in rather large hydrogel and calculating the value of diffusion coefficient from local measurements arises questions. In FCS, confocal volume is narrow and results from local movements are interpreted as diffusion in the whole hydrogel material. FRAP measurement results are obtained in ROI, the 2D detecting area where photobleaching is performed and movements in depth direction not captured. Additionally, sensors are detecting the local concentration and diffusion is simulated from those sampling points. Even though there can be multiple detection points which increase the reliability, hydrogel structure is heterogenic, and molecules might be stirring inside a certain pore and moving therefore very slowly along with diffusion gradient. That local movement would not simulate the diffusion mobility through the hydrogel sample. However, as in fcsSOFI, the local movement of probe molecules can particularly give information about the pore structure and that could be advanced in structure characterization.

Fluorescence methods widely used fluorescent dyes in detecting the diffusion behaviour and especially FITC-dextran in various sizes were used to estimate mobility. Fluorescence dyes are thought as inactive additive agents to the body protein or molecule and FITC dextran can be used to model the diffusion of proteins in different sizes. However, as discussed, the interactions between solute molecule and polymer network along with aggregation of solute molecules decrease the rate of diffusion. Additionally, electrochemical attraction forces can have negative impact on mobility. Interactions depend on the chemical nature of interacting molecules. Synthetic probe molecules are used instead of following the movements of glucose, or other necessary ingredients for cell cultures and therefore there might be alterations in interactions. Raman spectroscopy and NMR imaging can detect mobility without using fluorescence and therefore specific fluorescence

probes would not be needed. Finally, most of the methods in this literature review were performed without cell cultures and effects that cells have on reached diffusion properties could not be assessed. The number of possible interactions can increase in presence of medium, cellular consumption and metabolism, possible biodegradation of hydrogels and other in vitro processes. Furthermore, cells can proliferate to form plugs to prevent the diffusion. In conclusion, modelling diffusion with consideration of interactions that might have effect on diffusion can be complex but with many of the introduced methods, possible interactions between probe molecule and polymer network can be detected or excluded.

As discussed, sufficient availability of nutrients and necessary molecules is challenge in optimizing hydrogels for cell cultures and therefore diffusion characterization techniques are needed. Methods, such as FCS can reach the high level of accuracy and detect the movements of individual molecules. Along with detecting local diffusivities, imaging movements of diffusive molecules in the range of whole sample, reveals information about diffusion in larger scale. Both approaches can estimate the diffusion behaviour although there is a need for finding efficient method with necessary accuracy and decent costs. Accessible equipment and high-performance data-processing could be developed and comprehensively considered in creating mass transport testing methods. Deeper research on the current or new methods to reach the balance of efficiency, accuracy and reliability in mass transport characterization are needed to develop suitable hydrogel scaffolds for cell cultures.

REFERENCES

- [1] C. M. Kirschner and K. S. Anseth, "Hydrogels in healthcare: From static to dynamic material microenvironments," *Acta Mater.*, vol. 61, no. 3, 2013, doi: 10.1016/j.actamat.2012.10.037.
- [2] J. W. Haycock, "3D cell culture: a review of current approaches and techniques.," *Methods in molecular biology (Clifton, N.J.)*, vol. 695. 2011, doi: 10.1007/978-1-60761-984-0_1.
- [3] L. L. Hench and J. R. Jones, *Biomaterials, artificial organs and tissue engineering*. Woodhear Publishing, 2005.
- [4] M. Razavi, *Frontiers in Biomaterials: Biomaterials for Tissue Engineering*, 4th ed. Bentham Science Publishers, 2017.
- [5] E. M. Ahmed, "Hydrogel: Preparation, characterization, and applications: A review," *Journal of Advanced Research*, vol. 6, no. 2. 2015, doi: 10.1016/j.jare.2013.07.006.
- [6] S. Mishra, P. Rani, G. Sen, and K. P. Dey, *Hydrogels: Recent Advances Chapter 6 Preparation, Properties and Application of Hydrogels: A Review*. 2018.
- [7] N. Zoratto and P. Matricardi, "Semi-IPN- and IPN-based hydrogels," in *Advances in Experimental Medicine and Biology*, vol. 1059, 2018.
- [8] V. S. Raghuwanshi and G. Garnier, "Characterisation of hydrogels: Linking the nano to the microscale," *Advances in Colloid and Interface Science*, vol. 274. 2019, doi: 10.1016/j.cis.2019.102044.
- [9] F. Andrade, M. M. Roca-Melendres, E. F. Durán-Lara, D. Rafael, and S. Schwartz, "Review stimuli-responsive hydrogels for cancer treatment: The role of ph, light, ionic strength and magnetic field," *Cancers*, vol. 13, no. 5. 2021, doi: 10.3390/cancers13051164.
- [10] N. A. Stocke, X. Zhang, J. Z. Hilt, and J. E. DeRouchey, "Transport in PEG-Based Hydrogels: Role of Water Content at Synthesis and Crosslinker Molecular Weight," *Macromol. Chem. Phys.*, vol. 218, no. 3, 2017, doi: 10.1002/macp.201600340.
- [11] E. Nagy, *Basic equations of mass transport through a membrane layer*, 2nd ed. Elsevier, 2018.
- [12] S. H. Gehrke, J. P. Fisher, M. Palasis, and M. E. Lund, "Factors determining hydrogel permeability," in *Annals of the New York Academy of Sciences*, 1997, vol. 831, doi: 10.1111/j.1749-6632.1997.tb52194.x.
- [13] B. Amsden, "Solute diffusion within hydrogels. Mechanisms and models," *Macromolecules*, vol. 31, no. 23, 1998, doi: 10.1021/ma980765f.
- [14] S. Matsukawa, D. Sagae, and A. Mogi, "Molecular diffusion in polysaccharide gel systems as observed by NMR," *Prog. Colloid Polym. Sci.*, vol. 136, 2009, doi: 10.1007/2882_2009_24.
- [15] J. Balch and C. Guéguen, "Effects of molecular weight on the diffusion coefficient of aquatic dissolved organic matter and humic substances," *Chemosphere*, vol. 119, 2015, doi: 10.1016/j.chemosphere.2014.07.013.
- [16] C. P. Goodrich, M. P. Brenner, and K. Ribbeck, "Enhanced diffusion by binding to the crosslinks of a polymer gel," *Nat. Commun.*, vol. 9, no. 1, 2018, doi: 10.1038/s41467-018-06851-5.
- [17] H. Pohl, "What is the difference between fluorescence, phosphorescence and luminescence?" Enzo Life Sciences, 2019, [Online]. Available: <https://www.enzolifesciences.com/science-center/technotes/2019/december/what-is-the-difference-between-fluorescence-phosphorescence-and-luminescence?/>.
- [18] U. Kubitscheck, *Fluorescence Microscopy: From Principles to Biological Applications: Second Edition*, 2nd ed. Wiley-VCH, 2017.
- [19] A. M. Soto *et al.*, "Optical Projection Tomography Technique for Image Texture and Mass Transport Studies in Hydrogels Based on Gellan Gum," *Langmuir*, vol. 32, no. 20, 2016, doi: 10.1021/acs.langmuir.6b00554.
- [20] S. Prasad and R. Swaminathan, "Measuring the diffusion of fluorescent dye or protein inside living cells," *Curr. Sci.*, vol. 105, no. 11, 2013.
- [21] M. H. Hettiaratchi *et al.*, "A rapid method for determining protein diffusion through hydrogels for regenerative medicine applications," *APL Bioeng.*, vol. 2, no. 2, 2018, doi: 10.1063/1.4999925.

- [22] H. C. Ishikawa-Ankerhold, R. Ankerhold, and G. P. C. Drummen, "Advanced fluorescence microscopy techniques-FRAP, FLIP, FLAP, FRET and FLIM," *Molecules*, vol. 17, no. 4. 2012, doi: 10.3390/molecules17044047.
- [23] N. R. Richbourg and N. A. Peppas, "High-Throughput FRAP Analysis of Solute Diffusion in Hydrogels," *Macromolecules*, vol. 54, no. 22, 2021, doi: 10.1021/acs.macromol.1c01752.
- [24] A. Avendano *et al.*, "Integrated Biophysical Characterization of Fibrillar Collagen-Based Hydrogels," *ACS Biomater. Sci. Eng.*, vol. 6, no. 3, 2020, doi: 10.1021/acsbio.3b01873.
- [25] J. Karvinen, T. O. Ihalainen, M. T. Calejo, I. Jönkkäri, and M. Kellomäki, "Characterization of the microstructure of hydrazone crosslinked polysaccharide-based hydrogels through rheological and diffusion studies," *Mater. Sci. Eng. C*, vol. 94, 2019, doi: 10.1016/j.msec.2018.10.048.
- [26] D. Wöll, "Fluorescence correlation spectroscopy in polymer science," *RSC Advances*, vol. 4, no. 5. 2014, doi: 10.1039/c3ra44909b.
- [27] L. Yu *et al.*, "A Comprehensive Review of Fluorescence Correlation Spectroscopy," *Frontiers in Physics*, vol. 9. 2021, doi: 10.3389/fphy.2021.644450.
- [28] S. P. Zustiak, H. Boukari, and J. B. Leach, "Solute diffusion and interactions in cross-linked poly(ethylene glycol) hydrogels studied by Fluorescence Correlation Spectroscopy," *Soft Matter*, vol. 6, no. 15, 2010, doi: 10.1039/c0sm00111b.
- [29] X. Zhang, J. Hansing, R. R. Netz, and J. E. Derouchey, "Particle transport through hydrogels is charge asymmetric," *Biophys. J.*, vol. 108, no. 3, 2015, doi: 10.1016/j.bpj.2014.12.009.
- [30] L. Kisley *et al.*, "Characterization of Porous Materials by Fluorescence Correlation Spectroscopy Super-resolution Optical Fluctuation Imaging," *ACS Nano*, vol. 9, no. 9, 2015, doi: 10.1021/acsnano.5b03430.
- [31] S. Yoshida, W. Schmid, N. Vo, W. Calabrese, and L. Kisley, "Computationally-efficient spatiotemporal correlation analysis super-resolves anomalous diffusion," *Opt. Express*, vol. 29, no. 5, 2021, doi: 10.1364/oe.416465.
- [32] J. Sharpe, "Optical Projection Tomography," *Annu. Rev. Biomed. Eng.*, vol. 6, no. 1, pp. 209–228, Aug. 2004, doi: 10.1146/annurev.bioeng.6.040803.140210.
- [33] A. E. Donius, S. V. Bougoin, and J. M. Taboas, "FRET imaging in three-dimensional hydrogels," *J. Vis. Exp.*, vol. 2016, no. 114, 2016, doi: 10.3791/54135.
- [34] K. J. Son, D. S. Shin, T. Kwa, Y. Gao, and A. Revzin, "Micropatterned sensing hydrogels integrated with reconfigurable microfluidics for detecting protease release from cells," *Anal. Chem.*, vol. 85, no. 24, 2013, doi: 10.1021/ac402660z.
- [35] L. Figueiredo *et al.*, "Assessing glucose and oxygen diffusion in hydrogels for the rational design of 3D stem cell scaffolds in regenerative medicine," *J. Tissue Eng. Regen. Med.*, vol. 12, no. 5, 2018, doi: 10.1002/term.2656.
- [36] J. Demol, D. Lambrechts, L. Geris, J. Schrooten, and H. Van Oosterwyck, "Towards a quantitative understanding of oxygen tension and cell density evolution in fibrin hydrogels," *Biomaterials*, vol. 32, no. 1, 2011, doi: 10.1016/j.biomaterials.2010.08.093.
- [37] J. R. Ferraro, K. Nakamoto, and C. W. Brown, "Basic Theory," in *Introductory Raman Spectroscopy*, 2nd ed., Elsevier, 2003.
- [38] "What is Raman Spectroscopy?" Edinburg Instruments, 2022, [Online]. Available: <https://www.edinst.com/blog/what-is-raman-spectroscopy/>.
- [39] J. Zini *et al.*, "Drug diffusivities in nanofibrillar cellulose hydrogel by combined time-resolved Raman and fluorescence spectroscopy," *J. Control. Release*, vol. 334, 2021, doi: 10.1016/j.jconrel.2021.04.032.
- [40] I. L. Pykett *et al.*, "Principles of nuclear magnetic resonance imaging," *Radiology*, vol. 143, no. 1. 1982, doi: 10.1148/radiology.143.1.7038763.
- [41] Y. E. Shapiro, "Structure and dynamics of hydrogels and organogels: An NMR spectroscopy approach," *Progress in Polymer Science (Oxford)*, vol. 36, no. 9. 2011, doi: 10.1016/j.progpolymsci.2011.04.002.
- [42] D. Sandrin *et al.*, "Diffusion of macromolecules in a polymer hydrogel: From microscopic to macroscopic scales," *Phys. Chem. Chem. Phys.*, vol. 18, no. 18, 2016, doi: 10.1039/c5cp07781h.

APPENDIX A: TABLE OF CHARACTERIZATION METHODS

Table 1: Mapped characterization methods with advantages and disadvantages. Abbreviations of molecules and materials expressed in the table are explained below:

*FITC-dextran	Fluorescein isothiocyanate-dextran,
*FITC-PEG	Fluorescein isothiocyanate-poly(ethylene glycol)
*BSA-TRITC	Tetramethyl rhodamine isothiocyanate bovine serum albumin
*R6G	Rhodamine 6G
*EGFP	Enhanced green fluorescent protein
*BSA	Bovine serum albumin
*Ig	γ -globulin
*R110	Rhodamine 110
*A488	Alexa Fluor 488
*BMP-2	Bone morphogenic protein 2
*IgG	Human immunoglobulin G
* α CT	Bovine alpha-chymotrypsin
*FLU	Fluorescein
*TMR	Tetramethyl rhodamine
*PVA	Poly(vinyl alcohol)
*HA	Hyaluronan
*PEG	Poly(ethylene glycol)
*PAAm	Polyacrylamide
*Si-HPMC	Silicated hydroxypropyl-methylcellulose
*GG	Gellan gel
*ANFC	Anionic native nanofibrillated cellulose

Reference	Diffusive molecule	Hydrogel	Method(s)	Considered parameters on diffusion behavior	Detection site for diffusion probe	Advances	Possible disadvantages
Nathan and Peppas	Fluorescein, FITC-dextran, FITC-PEG*	PVA*	FRAP	Mesh radius, polymer volume fraction, hydrodynamic radius, immobilization	ROI	Automated data analysis, structure-diffusivity analysis	Detecting movements in 2D, reliability of generalizing local movements to diffusion in the whole hydrogel
Karvinen et al.	FITC-dextran	PVA/HA*	FRAP	Viscoelasticity, mesh size, crosslinking density, average molecular weight	ROI	Versatile preparation of hydrogels with hydrazone crosslinking, rheology-diffusivity analysis	Detecting movements in 2D, reliability of generalizing local movements to diffusion in the whole hydrogel
Avendano et al.	BSA-TRITC*	Collagen I	FRAP, fluorescence intensity for hydraulic permeability studies	Hydraulic permeability of BSA-TRITC, fiber radius and alignment, pore size	ROI	Structure-diffusivity analysis with hydraulic pressure studies	Detecting movements in 2D, reliability of generalizing local movements to diffusion in the whole hydrogel
Zustiak et al.	R6G, EGFP, BSA, Ig*	PEG*	FCS, protein assay in protein release	Swelling, mesh size, hydrodynamic radius, solute concentration, polymer density	Confocal volume, released protein concentration in solute	Validating FCS with release studies, studying movements in level of individual molecule	Reliability of generalizing local movements to diffusion in the whole hydrogel
Zhang et al.	R110, R6G, A488, R-phycoerythrin*	PEG, uncharged and charged dextran solutions	FCS	Charge of diffusive molecule and gel	Confocal volume	Charge studies, studying movements in level of individual molecule	Reliability of generalizing local movements to diffusion in the whole hydrogel
Hettiaratchi et al.	BMP-2, BSA, IgG, α CT*	Alginate, collagen, PEG	Fluorescence intensity for mobility studies	Polymer concentration	Fluorescence intensity in the whole hydrogel sample	Simple procedure and instrumentation	Detecting movements in large size scale
Sandrin et al.	Unlabelled and labelled dextrans: FLU, A488, TMR*	PAAm*	FCS, MTI, NMR	Hydrodynamic radius, molecular mass, pore size, polymer volume factor, interactions between probe and polymer	FCS: confocal volume, MTI: fluorescence intensity in the whole sample, NMR: local radiofrequency pulses	Validation of methods with comparison between different size-scale methods	NMR: water sensitivity and lower accessibility with equipment
Figueiredo et al.	Glucose, Oxygen	SI-HPMC*	Glucose sensor, fluorescent oxygen sensor	Oxygen and glucose permeability, elasticity, polymer concentration, mesh size	Local concentrations	In vitro evaluation (human adipose derived stem cells (hASCs)), label-free	Invasive
Demol et al.	Oxygen	Fibrin	Oxygen microsensor	Cell viability, oxygen consumption	Local concentrations or partial pressures	In vitro evaluation (human periosteum derived cells (hPDCs)), label-free	Invasive
Matsukawa et al.	Dendrimer, pullulan	Agar, gellan gel	PFGE-NMR	Temperature-dependence, mesh size	Local radiofrequency pulses	Temperature studies, gelation process studies, label-free	NMR: water sensitivity and lower accessibility with equipment
Soto et al.	FITC-dextran	GG*	OPT	Microstructure, heterogeneity, crosslinking density and method	Fluorescence intensity in imaging area	Hydrated environment, simple procedure and instrumentation	Detecting movements in large size scale
Zini et al.	Vitamin C, metronidazole	ANFC*	Raman spectroscopy (CMOS-SPAD -sensor), FLIM	Raman vibrations, intermolecular interactions	Local Raman scattering and fluorescence decay	Insensitivity to water, label-free	Raman spectroscopy: Invasive